# Characterization of the 2-Phase Turning Response of Madagascar Hissing Cockroach Biobots to Antennal Stimulation

Stefanie Jane Panzenhagen

**Characterization of the 2-Phase Turning Response of Madagascar Hissing Cockroach Biobots to Antennal Stimulation**

A Thesis

Submitted to the Faculty

of

Rose-Hulman Institute of Technology

by

Stefanie Jane Panzenhagen

In Partial Fulfillment of the Requirements for the Degree

of

Master of Science in Biomedical Engineering

November 2019

**DEFENSE REPORT**

**ROSE-HULMAN INSTITUTE OF TECHNOLOGY**

**Final Examination Report**

Stefanie Panzenhagen

Name

Biomedical Engineering

Graduate Major

Thesis Title    Characterization of the 2-Phase Turning Response of Madagascar Hissing Cockroach

Biobots to Antennal Stimulation

**DATE OF EXAM:**    September 6, 2019

**EXAMINATION COMMITTEE:**

| | Thesis Advisory Committee | Department |
|---|---|---|
| Thesis Advisor: | Alan Chiu | BBE |
| | William Weiner | BBE |
| | Deborah Walter | ECE |
| | | |
| | | |

**PASSED** _____X_____          **FAILED** _____

# ABSTRACT

Panzenhagen, Stefanie Jane

M.S.B.E.

Rose-Hulman Institute of Technology

November 2019

Characterization of the 2-Phase Turning Response of Madagascar Hissing Cockroach Biobots to Antennal Stimulation

Thesis Advisor: Dr. Alan Chiu

Biobots are living insects that are controlled via neurostimulation applied through implanted electrodes and have a variety of potential applications such as search and rescue operations. Madagascar Hissing Cockroaches (MHCs) are commonly used as biobots; however, their use remains under investigation due to lack of a comprehensive motion profile in response to neurostimulation, which makes consistent control a challenge. MHC biobots often exhibit a 2-phase turning response to antennal stimulation, with an initial turn (primary) in the desired direction followed by a "corrective" turn (secondary) in the undesired direction. The purpose of this research is to characterize the 2-phase turning response of MHC biobots to antennal stimulation. Electrodes were implanted into the antennae of MHC biobots (n=20), and antennae of each subject were stimulated 40 times using a duty cycle of 50%, frequency of 125 Hz, and four sets of stimulus voltages and durations: 1 V and 0.5 s, 3 V and 0.5 s, 1 V and 1.5 s, and 3 V and 1.5 s. Modulation of stimulation voltage and duration did not significantly affect the responsiveness, direction of, or magnitude of turn angles. The direction of primary turns were found to be controlled in 88% of subjects, while the direction of secondary turns were able to be controlled in only 53% of subjects, which demonstrates that MHC biobots are able to be consistently controlled during the primary turn but not during the secondary turn. A histogram

of the magnitude of secondary turns is centered approximately at 0°, which demonstrates that the secondary turn is likely when the cockroach regains control of its motion rather than a "corrective" turn as noted in previous studies. To improve MHC biobot technology, researchers could limit the amount of time between stimuli or introduce a feedback system where actual turn angle is measured, and stimuli are applied when the MHC biobot begins turning in the undesired direction.

**DEDICATION**

I dedicate this work to my parents, who have taught me by example to persist.  It is your

unwavering faith in me that makes me the woman I am today.

# ACKNOWLEDGEMENTS

I extend sincere gratitude to the following:

Dr. Alan Chiu for his guidance, expertise, passion for research, humor, and willingness to put up with me for the past 5 years. Thank you for taking me under your wing and for your genuine interest in this research.

Kierra Rogers, Michael Doyel, David Hughes, and Jan Mangawang for assisting me with experiments this year. Thank you for your help and great attitudes throughout the process.

Dr. William Weiner for his guidance, expertise, and support. Thank you for guiding me in pursuing this degree, as well as guiding me in my career path.

Dr. Walter, for bringing her expertise to this thesis. Thank you for your great ideas and sacrificing time to help me.

Dr. Diane Evans, Dr. Eric Reyes, Dr. Jameel Ahmed, Dr. Renee Rogge, Dr. Emma Dosmar, Dr. Glen Livesay, Dr. Peter Coppinger, Dr. Stephanie Hill, and Lisa Knott, for supporting me throughout my time at Rose-Hulman. Your passion for engineering is truly contagious.

Ray Bland, for sacrificing his time to make this thesis possible.

Claire Raffin, for traversing through this year with me and being a nonstop source of laughter.

**TABLE OF CONTENTS**

# LIST OF FIGURES

# LIST OF TABLES

# LIST OF ABBREVIATIONS

| | |
|---|---|
| Biobots | Biological Robots |
| MHC | Madagascar Hissing Cockroach |

## 1.  INTRODUCTION

Biological robots, otherwise known as biobots, are living insects that are controlled via neural stimulation applied through implanted electrodes.  Biobots often carry lightweight electronic backpacks that receive remote signals and provide appropriate stimuli via the implanted electrodes to control insect motion and behavior [1].  Their low power consumption and innate ability to navigate rough terrain make biobots an attractive technology for use in various applications, such as search and rescue and reconnaissance [2].  Madagascar Hissing Cockroaches (MHCs) are insects commonly used in biobot applications due to their relatively large size of 2-3 inches, ability to carry large loads their body weight, and lifespan of 2-5 years [3].

Currently, low response rates, where responsiveness is defined as the ability to induce MHC motion in the desired direction via neurostimulation, is a major limitation that needs to be addressed before MHC biobots can be implemented commercially.  For instance, MHC biobots have historically demonstrated response rates of 10-50% to stimulation of sensory neurons in the antennae [3, 4].  More recent studies have demonstrated response rates of greater than 70% using biphasic electrical stimulation [5].  Still, before biobots can be fully implemented outside of a research setting, it is essential that appropriate measures be taken in order to improve response rates to neurostimulation.

Biobots are also still under investigation due to lack of a comprehensive motion profile in response to neurostimulation.  One study noted that MHC biobots often exhibit a two-phase turning response to antennal stimulation [5]. The initial turn occurs almost immediately upon stimulation in the direction contraversive to the stimulus, while a second turn may occur slightly after the termination of stimulation in the ipsiversive direction.  In some cases, these secondary

turns may even be larger than the first, causing the end result to be a turn in the unintended direction. However, the characterization of the motion responses of MHC biobots to neurostimulation has been limited to the initial turn. Before MHC biobots can be effectively and consistently utilized, it is necessary to develop a comprehensive motion profile in response to antennal stimulation.

The purpose of this thesis is to characterize the two-phase turning response of the MHC biobot to electrical stimulation of the antennae. More specifically, it aims to investigate how modulation of stimulation amplitude and duration affect responsiveness and turning angles of MHC biobots. The ultimate goal of this research is to gain more reliable control over MHC biobot motion and bring the technology closer to full implementation.

## 2. BACKGROUND INFORMATION

### 2.1 Biological Robots

Because biobots are living insects, they have the ability to navigate rough terrain easily and squeeze into small places [1]. These characteristics make biobots useful in many applications including, but not limited to, search and rescue, building inspection, mapping unknown territory, mining, and reconnaissance [6]. For instance, researchers have demonstrated that MHC biobots can be autonomously guided to a sound source using onboard microphones [7]. Setting a swarm of these biobots loose in, for example, the rubble of a fallen building after an earthquake may be a promising method to find survivors quickly. With insects' innate ability to fit into small crevices and openings, it is possible that biobots would be able to inspect pipes in hard to reach places in buildings. Furthermore, it is likely possible to map a dangerous, unknown area by equipping biobots with specific sensors and releasing them near the area [1]. For instance, biobots could be equipped with altimeters, which could send elevation data back to the user via radio frequency waves [8]. Biobots have also begun to be used in the promotion of youth interest in science. Backyard Brains' RoboRoach is currently the only commercially available biobot with the goal of teaching students about advanced neurotechnologies [9].

Many of the applications of biobots listed above could be accomplished by the use of miniature robots. However, miniature robots come with their own set of challenges. Their main drawback is that they use up to 1000x more power than biobots due to the fact that miniature robots' motion is powered by batteries whereas short electrical stimuli are the only power requirement for biobots [10, 11, 12]. On the other hand, the motion of living biobots is powered by the intake of water, air, and food. To put this in perspective, a miniature drone may only have enough battery to fly 20 minutes while a winged-biobot may be able to fly for many hours.

Another shortcoming of using miniature robots is that many sensors would be required to allow the robots to adapt to a dynamic environment, which would inevitably increase the size and complexity of the robot [13]. Currently, autonomous navigation at this scale in dynamic environments is not well understood. Biobots, on the other hand, have innate sensory systems which allow them to respond to their environment accordingly. Furthermore, controlling locomotion in robots at minuscule scales is difficult and requires advanced software. Similar to their sensory systems, biobots also have innate neuromuscular systems.

Many species of insects, including the tobacco hawk moth (*Manduca sexta*) [14], the rhinoceros beetle (*Mecynorhina torquata*) [15], the American grasshopper (*Schistocerca americana*) [16], various species of dragonflies (*Anisoptera*) [17], and various species of cockroaches including the American cockroach, the discoid cockroach, and the Madagascar Hissing Cockroach (*Periplaneta Americana, Blaberus discoidalis,* and *Gromphadorhina portentosa*) [18, 5], have been investigated for use as biobots (shown in Figure 1 below). The optimal insect for biobot applications depends on the intended use of the biobot. Dragonflies, moths, and flying beetles offer significant advantages when compared to cockroaches and grasshoppers in settings that require biobot flight. On the other hand, the large size and heavy payload of cockroaches are more advantageous in applications that require larger sensors. Still, more species of insects are currently being investigated as potential biobots.



**Figure 1.** Examples of insects used in biobot applications include (a) dragonflies (*Anisoptera*) [17], (b) the tobacco hawk moth (*Manduca sexta*) [19], and (c) the rhinoceros beetle (*Mecynorhina torquata*) [20].

2.2 Madagascar Hissing Cockroaches

Madagascar Hissing Cockroaches, otherwise known as *Gromphadorhina portentosa,* have several characteristics that make them the ideal candidates in biobot applications. Most importantly, they are one of the largest species of cockroaches with a length of approximately 50-75 mm [21]. This allows them to carry electronic backpacks, as seen in Figure 2, without significant change to their normal gait. Additionally, MHCs are readily available, easy to take care of in a laboratory setting, and have a relatively long lifespan of approximately 2 years. With regards to motion, their slow and controlled maneuvers allow humans to steer them as biobots in real-time. They are also excellent climbers and robust insects in general [5].
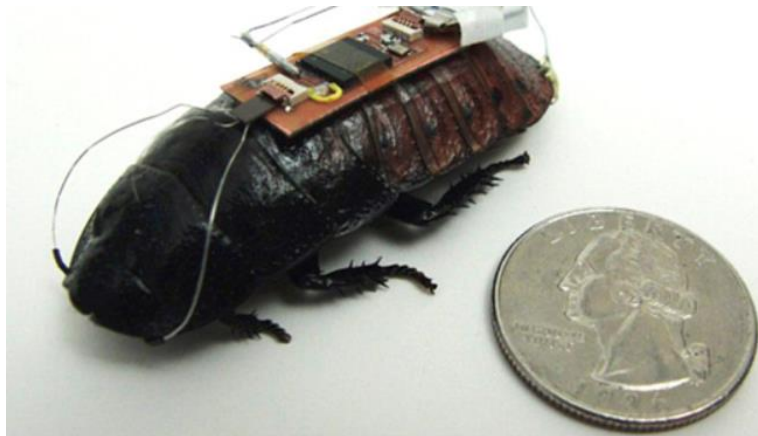


**Figure 2.** A Madagascar Hissing Cockroach with electrodes implanted in its antennae and cerci. It carries a lightweight electronic backpack that receives remote signals and stimulates the electrodes [22].

However, the use of MHCs as biobots has its limitations. First, as tropical creatures, they prefer temperatures of 24 - 32°C [23]. At less than 18°C, MHCs become inactive as their motion slows [24]. Their inactivity in cold temperatures may add challenges to the implementation of MHC biobot technology, as one proposed application for biobots is in search and rescue endeavors. Furthermore, as ectotherms, MHCs physically tire easily. For this reason, it is necessary to give MHC biobots rest during sessions of neurostimulation.

In order to understand how MHC biobot technology can be improved, it is first essential to understand the anatomy of an MHC. Main features of MHC anatomy are shown in Figure 3. Important outer features on the MHC include the antennae, pronotum, thorax, abdomen, selerites, and cerci. On MHC legs, distinguishing features include the coxa, the trochanter, the femur, the tibia, and the tarsi [25].
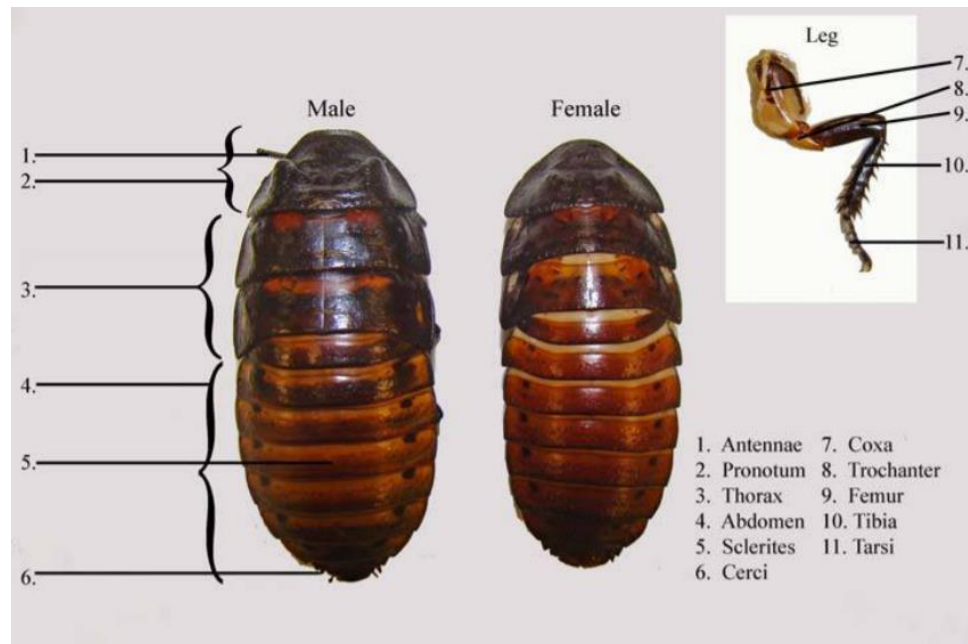


**Figure 3.** Main features of Madagascar Hissing Cockroach anatomy [25].

The antennae, shown in Figure 4, are multifunctional appendages that provide sensory feedback for a multitude of senses, including olfactory, humidity, thermal, tactile, and gustatory. Specifically, it is the tactile sense of the antenna that provides the perception of physical objects. This tactile sense is made possible by many mechanoreceptors on the surface of the antennae. The majority of studies conducted on cockroach antennae have utilized the American cockroach as a model [26]; however, it is likely that MHC antennae function very similarly based on the similarities between the 2 species. When one antenna of an MHC is stimulated, the MHC perceives that a physical object is touching that antenna. The MHC will then move in the contralateral direction of the perceived object.
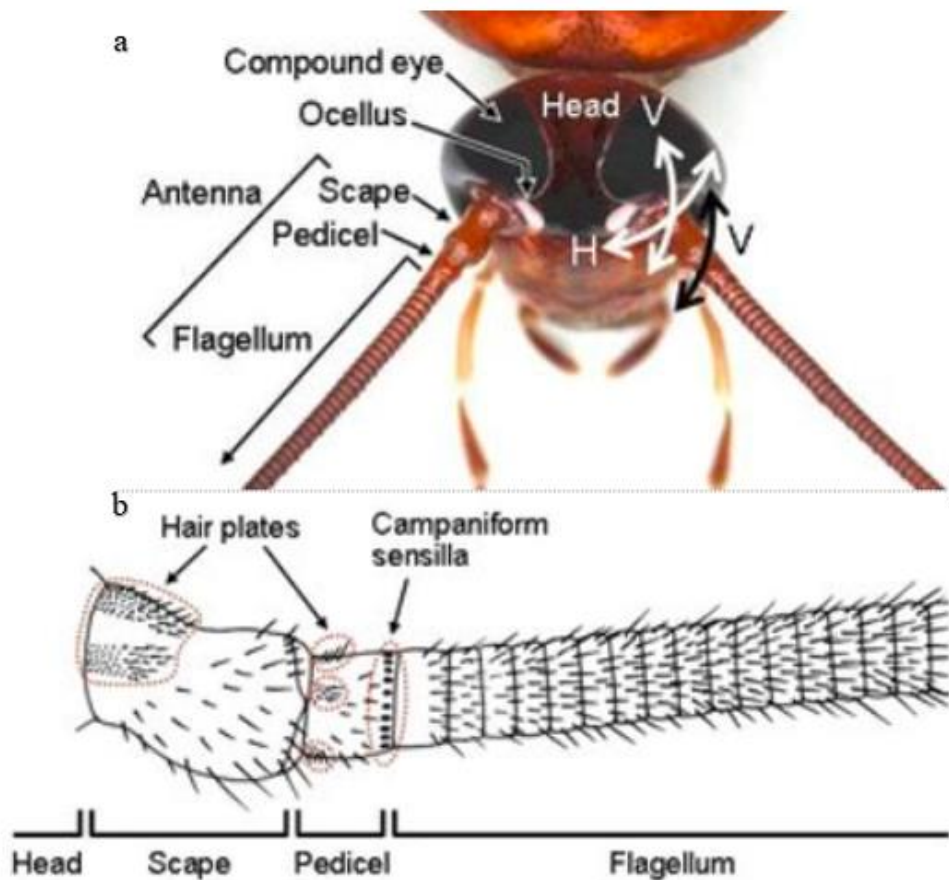
**Figure 4.** (a) Antenna of an American cockroach. (b) Lateral view of an American cockroach antenna [26].

The cerci, shown in Figure 3 on the end of the abdomen, act as sensory appendages that are sensitive to vibrations in the air or ground. Being covered with wind-sensitive hairs, cerci in most species of cockroach are able to sense objects or organisms rapidly approaching from behind. The cerci are connected directly to abdominal nerve ganglia, which control the legs of cockroaches. When the cerci are stimulated via vibrations in the air or ground, the escape response is initiated where the cockroach begins to run from the stimulus rapidly [27]. However, MHCs do not exhibit the same escape response as other species of cockroach in response to wind [28]. Despite their lack of escape response in response to wind stimuli, previous studies have demonstrated that stimulation of MHC cerci still generates a rapid forward running response [3].

2.3 Electrode Placement

Biobot motion can be directed via the stimulation of sensory pathways or motor pathways. Different sensory pathways can theoretically be used to direct biobot motion. The goal of using a sensory pathway is to cause a biobot to sense something not actually present, which may lead the biobot to move in the desired direction. Motor pathways may also be used to direct biobot motion; however, this requires control of multiple motor neurons, which is more complex and difficult to implement on an insect model.

Though stimulating the eyes or sense of smell of an MHC biobot may be an option for directing MHC biobot motion, these methods are logistically difficult and require complex stimulus electronics. These methods also require detailed knowledge of MHC anatomy and physiology, which is not readily available. An advantageous alternative pathway is the stimulation of MHC biobot antennae. As MHC antennae provide sensory feedback, stimulating one antenna essentially "tricks" the MHC biobot into sensing an obstacle that is not there, causing the MHC biobot to turn in the contraversive direction of stimulation. The cerci are also involved in providing sensory feedback to MHCs. Stimulation of both the cerci and antennae causes MHC biobots to move forward while turning, as is consistent with a cockroach's escape response. This pathway was proven to be moderately successful in 1998 when Moore et al. was able to direct MHC biobot motion with a low response rate of 10% [3]. In previous MHC biobot studies, a ground electrode is placed in the abdomen of the MHC, and stimulation electrodes are inserted into the antennae. If cerci are also stimulated, stimulation electrodes are inserted into the cerci [5]. An example of an MHC biobot with electrodes implanted in the antennae, cerci, and abdomen is shown in Figure 5. Stimulation of the antennae alone, as well as the antennae

and cerci simultaneously, are currently the only pathways that have been successfully

implemented in MHC biobots.



**Figure 5.** A Madagascar Hissing Cockroach biobot with electrodes implanted in its antennae, cerci, and abdomen [5].

Motor neuron pathways may also be used to direct biobot motion. With the motor neuron

pathway, the goal is to stimulate neurons that cause certain muscles to either move or cease

motion. One potential method involving stimulation of motor neurons includes the stimulation

of prothoracic ganglia in cockroaches. Depending on which ganglia are stimulated, a particular

cockroach leg becomes out of phase with the gait of the other legs as the cockroach runs. This

causes the cockroach to turn in the desired direction [18]. An example of electrode placement

and a neural map of a discoid cockroach is shown in Figure 6.

brain

electrodes

*prothoracic ganglion:* controls raw movements of the first pair of legs. Electrodes are inserted into the ganglion through the pronotum.
*mesothoracic ganglion:* controls raw movements of second pair of legs and forewings

thoracic ganglia

*metathoracic ganglion:* controls raw movements of the third pair of legs and hind wings

abdominal ganglia

*cercial ganglion:* receives information from the cerci and triggers the signal that initiates the escape reaction

**Figure 6.** A neural map of a discoid cockroach, showing where electrodes would stimulate the prothoracic ganglia in order to direct discoid cockroach biobot motion [18].

The motor neuron stimulation method has not yet been successfully implemented in MHC biobots; however, it has been successfully implemented using American and discoid cockroaches (*Periplaneta americana* and *Blaberus discoidalis)* with relatively high repeatability of 60% [18].  Because of the anatomical similarities of MHCs to American and discoid cockroaches, it is highly likely that this method could be used to direct biobot motion successfully in MHCs.  However, the neuroanatomy of MHCs have not been studied as extensively as American and discoid cockroaches.  Before this method can be implemented, it is necessary to create a neural map for the species similar to the neural map shown in Figure 6.

2.4 Electrical Stimulus Parameters

Before MHC biobots can be fully implemented on a commercial scale, it is necessary to determine the ranges of electrical pulse stimulus parameters that exhibit responses and evaluate how changing those parameters affects the subsequent biobot motion. Specifically, it is necessary to determine the effects of monophasic v. biphasic stimuli and whether current-controlled or voltage-controlled is optimal. Furthermore, it is necessary to define effective ranges for stimulus amplitude, stimulus frequency, stimulus duration, and duty cycle (see Figure 7). Previous studies have provided ranges for many stimulus parameters that were deemed effective at controlling MHC biobot motion. It is necessary to create a full motion profile in response to specific stimulus parameters.
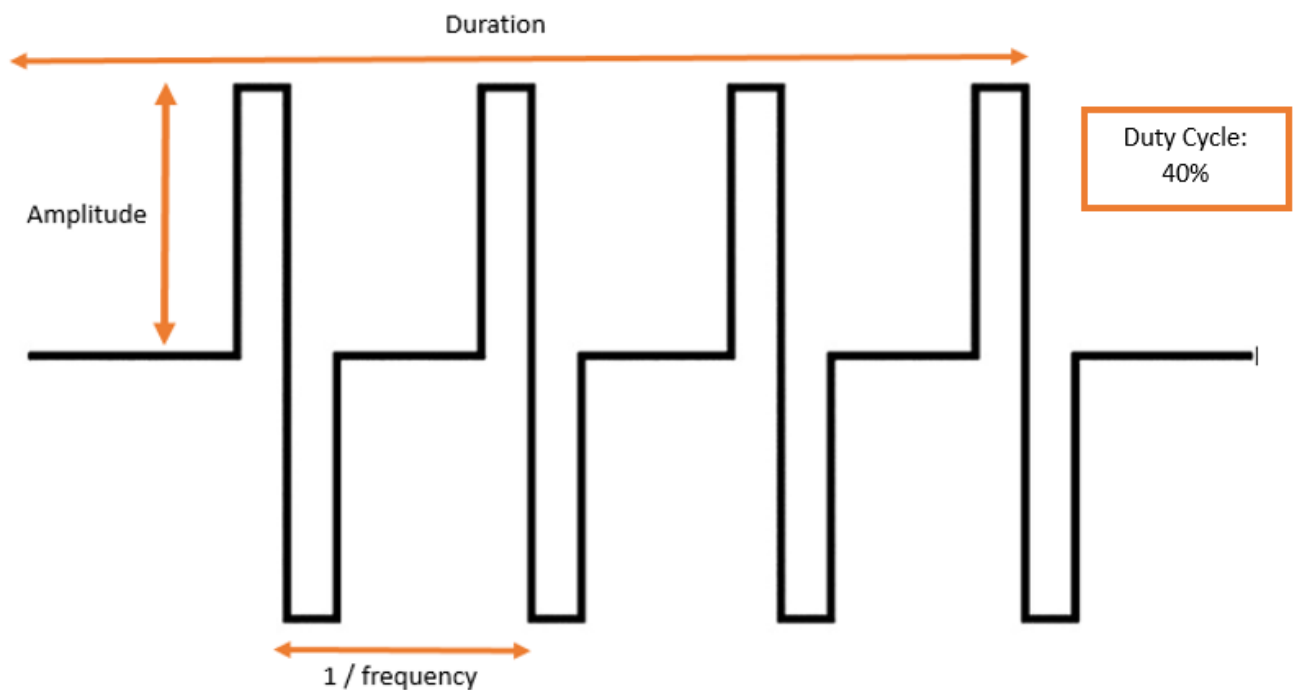


**Figure 7.** A biphasic pulse train with amplitude, frequency, duration, and duty cycle labeled.

Previous work has demonstrated that biphasic stimuli are much more effective at directing MHC biobot motion than monophasic stimuli [5]. Early research on MHC biobots used monophasic stimuli, which resulted in relatively low response rates of 10-45% [3]. However, newer research utilizing biphasic stimuli has demonstrated significantly higher response rates up to 75% [5]. Furthermore, biphasic stimuli applied to both the antennae and cerci was associated with higher levels of motion; in one study, 46.9% of subjects undergoing monophasic stimuli were deemed strong responders, while 59.4% of subjects undergoing biphasic stimuli were deemed strong responders, where strong responders were subjects that consistently responded with higher turn angles and distances [5]. In addition, biphasic pulses are known to cause lower amounts of cellular damage, as monophasic stimuli are associated with high charge densities that can cause tissue damage [29]. Another study found that biphasic voltage-controlled stimulation is more effective at generating action potentials in dissociated cultures of cortical neurons [30].

Previous work has also shown that voltage-controlled stimulation of MHC biobot antennae was associated with higher response rates when compared with current-controlled stimulation [5]. Most previous studies have utilized voltage-controlled stimulation strategies, as voltage-controlled neurostimulators require more simple electronics [3, 4, 5].

Pulse stimuli with amplitudes of ranges between 1-4 V, frequencies of ranges 50-300 Hz, and pulse durations of 0.25-1.5 s, have been successfully used to direct MHC biobot motion [5]. Higher amplitudes are associated with slightly slower turning motions. Frequency has not demonstrated a significant effect on turning motion. Longer pulse durations are associated with slightly higher turning angles. The mean turning angles under a variety of pulse parameters ranged from approximately 80°-150° [5]. One study determined that the optimal (based on the

highest response rate) pulse parameters were biphasic, 2 V, 50 Hz, 0.5 s voltage-controlled square pulses with 50% duty cycle [5]. These results were based on stimulation of both the antennae and cerci.

Previous work has described a 2-phase turning response to antennal stimulation, where an initial, or primary, turn in the contralateral direction of stimulation is observed followed by a "corrective," or secondary, turn in the ipsilateral direction of stimulation [5]. However, no studies have been conducted to measure the angle of the secondary turn or when the onset of the secondary turn occurs.

## 2.5 Habituation

Previous studies have demonstrated that MHC biobots often become habituated to neurostimulation of the antennae, meaning that the biobots would respond to neurostimulation less often, with shorter durations of subsequent motion, and with smaller turn angles [3, 4, 5]. As the antennae provide sensory feedback, MHCs over time are able to ignore them and depend on their other senses, such as the tiny sensory hairs on their legs. Most previous studies utilized monophasic stimuli, where response rates were relatively low and habituation occurred quickly (after approximately 40 trials). However, a more recent study demonstrated that only 2.9% of the subjects habituated to biphasic stimuli, while 31.3% of the subjects habituated to monophasic stimuli [5]. Therefore, biphasic stimuli are optimal and significantly reduce habituation.

## 2.6 Summary

In order to fully implement MHC biobots, it is necessary to create a full motion profile in response to neurostimulation. This motion profile should include the characterization of primary and secondary turns, including responsiveness, turn directions, and turn angles. Without the

characterization of the secondary turn, MHC biobot motion is difficult to effectively and reliably control.  Therefore, the purpose of this research is to characterize the 2-phase turning response of MHC biobots to antennal stimulation with varying stimulus parameters.  The greater goal of this research is to fully implement MHC biobots in a commercial setting, where the biobots can be used primarily in search and rescue applications.

**3. METHODS**

3.1 Overview

A total of 20 MHCs (17 male/3 female) were utilized in this study. Thin silver wires were implanted into the antennae and abdomen of each subject. After allowing at least 24 hours for recovery post-implantation, subjects underwent approximately 25-minute sessions of electrical stimulation to the antennae. Biphasic square pulse trains were applied to the antennae of each subject via a function generator set at varying voltages and durations. These conditions are shown in Table 2. The type of stimulus applied was randomized, and its application alternated between the left and right antenna. Each stimulation session lasted approximately 25 minutes.

MHC motion during and post-stimulation was captured via video recording. Linear motion data for both primary and secondary turns, including coordinates, distances traveled, velocities, and accelerations were extracted from the videos with Kinovea software (Kinovea beta release, Kinovea). Angular motion for both primary and secondary turns, including turning radii, turn angles, angular velocities, and angular accelerations were extracted from the videos with a combination of a custom Matlab program and Kinovea software.

More in-depth descriptions on methods involving the test subjects, stimulus electronics, the motion capture system, motion data extraction, further data processing, and statistical analyses used are found in the following sections. Section 3.2 provides information relating to the care and selection of MHC subjects. Section 3.3 details the technique used to implant electrodes into the MHC subjects. Section 3.4 details the design of the electronics used to apply stimuli to the MHC subjects. Section 3.5 describes the motion capture equipment and physical experimental setup. Section 3.6 demonstrates how linear and angular motion data was extracted

from video files. Section 3.7 describes further processing methods used to analyze the motion data. Finally, Section 3.8 explains the statistical analyses used to analyze data in this study.

3.2 Madagascar Hissing Cockroach Subjects & Care

MHCs were obtained (Carolina Biological) and housed in a 10-gallon tank with a screen cover at room temperature in a laboratory setting at Rose-Hulman Institute of Technology. An 8-watt heating pad (Reptitherm Undertank Heater, Zoomed) was applied to the side of the tank to maintain a temperature of 21°C-32°C, as MHCs prefer and are more active under higher temperatures [24]. The MHCs were given fresh water daily and fed lettuce and mandarin oranges twice a week. At the conclusion of the study, all MHCs were euthanized. Because *Gromphadorhina portentosa* is an invertebrate species that is not protected or endangered, no permissions were necessary to utilize them for this study. No permit was required to obtain this species in the state of Indiana. High ethical standards were followed throughout the duration of the study.

The weight of each subject was measured with a digital scale and recorded. The length, width, and height of each subject was measured and recorded with digital calipers. The sex of each subject was determined by the presence of or the lack of large horns on the pronotum, as male MHCs are known to exhibit large horns compared to the small bumps females exhibit [21]. Table 1 shows the means and standard deviations for size characteristics measured for all subjects. Each subject's individual size characteristics and sex can be found in Appendix A. Upon obtaining subjects 4 and 16, it was noted that both of their right antennae were not intact. In these cases, all 40 stimuli were applied to the remaining left antennae.

**Table 1.** Subject demographic data including the number of subjects, mean weight, mean length, mean width, mean height, and sex makeup.

| Number of subjects | Weight (Mean ± Standard Deviation) | Length (Mean ± Standard Deviation) | Width (Mean ± Standard Deviation) | Height (Mean ± Standard Deviation) | Sex (Males/Females) |
|---|---|---|---|---|---|
| 20 | 7.65 ± 1.04 g | 60.08 ± 4.07 mm | 22.83 ± 1.37 mm | 16.41 ± 0.82 mm | 17/3 |

3.3 Electrode Implantation

To create the electrodes for neurostimulation, three approximately 5-cm long strands of 0.005-in diameter non-insulated silver wire (A-M Systems) were soldered onto a 3-contact electrical header for each subject. An example of the electrodes and electrode header are shown in Figure 8. In order to anesthetize the insects, each subject was first placed into ice water in a cooler for approximately 5 minutes, ensuring that the dorsal side of the insect remained above water at all times as MHCs breathe through spiracles located in this region [31]. Because MHCs are ectothermic, reducing their temperature results in reduction of nervous and metabolic function which effectively anesthetizes the insects [32].
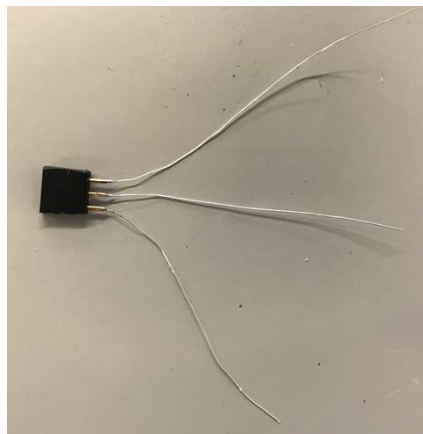


**Figure 8.** Electrode and electrode header.

After removing each subject from the ice water, each subject was placed on its ventral side and gently dried with a paper towel. In order to allow the glue to hold more easily, the thorax of each subject was gently sanded with sandpaper and cleaned of residue with a paper towel. 2-3 drops of superglue (Cyanoacrylate, The Original Super Glue Corporation) was applied to the sanded region of the thorax. The black electrical header was then immediately placed onto the glue, such that the protruding silver electrodes faced the anterior end of the insect. A hot-glue gun was used to secure the black electrical header on the medial and lateral sides, ensuring that the tip of the hot-glue gun did not touch the insect. The electrode header secured in place is shown in Figure 9.



**Figure 9.** Placement of the electrode header secured with glue on the thorax of a subject.

The subjects were placed back into ice water for approximately 5 minutes, again ensuring that the dorsal sides remained above water at all times. Once removed from the ice water, each subject was placed on its ventral side and again dried with a paper towel. Each antenna was then cut to a length of approximately 1 cm with a pair of dissection scissors. The outer silver wires were inserted into each antenna by about 1-2 mm. Small drops of superglue were applied to the wires just outside of the tips of the antenna, and the wires were then inserted further until noticeable resistance was felt; this step secures the wires in the antennae tightly due to the fact that superglue polymerizes once it contacts the MHCs' internal saline [32]. The subjects were

then turned, so they rested on their dorsal side. Using a hot-glue gun, the antennae themselves were glued to the pronotum of the cockroach. Special care was taken to ensure that the tip of the hot-glue gun did not touch the cockroaches and that no glue was applied to the cockroach's head.

The subjects were placed back on their ventral sides. A small insect pin was carefully pushed into the right side of the abdomen to create a small hole for the ground electrode. The hole was dabbed with a paper towel to remove any internal saline. The middle silver wire was inserted into the hole in the abdomen by approximately 1 mm. A drop of superglue was applied to the hole, and the wire was inserted further by approximately 5 mm. Figure 10 shows an MHC biobot with electrodes implanted into both antennae and abdomen.



**Figure 10.** A subject following implantation surgery, shown with thin silver wires implanted into its antennae and a wire implanted into the abdomen.

Following implantation surgery, single subjects were placed into a 3-gallon tank with a screen cover. This environment enabled that the insects with implanted wires did not burrow under or walk over each other, which maintained the integrity of the wires prior to any electrical stimulation. MHCs were allowed at least 24 hours in the 3-gallon tank to recover following

implantation surgery prior to a session of stimulation.  After sessions of stimulation, these subjects were placed back into the main 10-gallon tank.

### 3.4 Stimulus Electronics

A total of 40 125 Hz, 50% duty cycle, biphasic pulse trains were applied to the antennae of each subject with varying voltages and durations.  The stimulation voltages and durations are listed in Table 2.  Each antenna received five of each type of stimulus so that each subject received a total of 10 of each type of stimulus.

**Table 2.** Four sets of stimulus parameters used to stimulate 20 subjects' left and right antennae.  Each subject underwent 10 antennal stimuli in a given set of stimulus parameters.

|  | Pulse Stimulus Parameters Set #1 | Pulse Stimulus Parameters Set #2 | Pulse Stimulus Parameters Set #3 | Pulse Stimulus Parameters Set #4 |
|---|---|---|---|---|
| Voltage (V) | 1 | 3 | 1 | 3 |
| Duration (s) | 0.5 | 0.5 | 1.5 | 1.5 |

A function generator (Isolated Pulse Stimulator Model 2100, A-M Systems) was used to generate biphasic square pulse trains.  All pulse trains generated had a duty cycle of 50% and were at a frequency of 125 Hz or an inter-pulse period of 8 ms.  The function generator is shown in Figure 11, with an example amplitude and pulse train duration of 1 V and 0.5 s.  To change the duration of the pulse trains, the train burst width was modulated between 0.5 and 1.5 s.  To change the voltage of the pulse trains, the amplitude was modulated between 1 and 3 V.  Under pulse duration, the square setting denotes that all the pulse train generated for all stimuli was composed of square waves.  The pulse sign was set to biphasic for all stimuli.  A trigger was connected to the "TRIG" port on the function generator.  When the trigger was pressed, a pulse

train would be initiated with the parameters shown on the function generator. During each

stimulus, the green event light lit up.



**Figure 11.** The Isolated Pulse Stimulator Model 2100 (A-M Systems) was used to create biphasic pulse trains.

Alligator clip wires were inserted into the output and ground of the function generator.

The other ends of these wires were connected to 0.10-inch diameter PFA-coated platinum wires

(A-M Systems). These smaller wires were used due to their lightweight and flexibility, which

when attached to MHC biobots did not alter their normal gait. The tips of the thin platinum

wires were deinsulated using a blade. The thin platinum wires were soldered onto a short green

and orange breadboard wires, which corresponded with ground and power, respectively. These

breadboard wires were subsequently soldered onto electrical headers to allow for easier set-up

when connecting the subjects to the function generator. Three breadboard wires were inserted

into the electrical headers on each subject's thorax so that the wires were completely vertical.

The middle breadboard wire on each subject was inserted into the header corresponding with the

ground. If stimulating the left antenna, the subject's anatomical left breadboard wire was

inserted into the header corresponding with power. If stimulating the right antenna, the subject's

anatomical right breadboard wire was inserted into the header corresponding with power. Figure

12 shows an example of a subject with this electrical set-up.

**Figure 12.** A subject hooked up to the pulse generator with thin platinum wires, which minimizes the amount of tension placed on the subject. The green wire denotes ground, and the orange wire denotes the wire that provides the stimulus to the right antenna.

3.5 Experimental Set-Up & Motion Capture

The experimental set-up is shown in Figure 13. A 50 x 50-in foam pad was placed on the ground. A smartphone-holding tripod (50" Aluminum Camera Tripod, Acuvar) was placed on the edge of the pad. A smartphone was placed on the tripod, and the tripod was adjusted appropriately to capture the entire pad. Four meter sticks were placed in a square in the center of the pad, which allows for proper calibration during later data processing of the captured videos. The function generator was placed on the edge of the foam pad, which allowed for the smartphone to capture the green light, which indicated the start of a pulse train. To capture the subjects' motion responses to each stimulus, a video on the smartphone was collected for approximately 10 s for each stimulus. The trigger button was pressed to initiate a pulse train approximately 1 s after the start of video capture. The motion capture videos were subsequently transferred and analyzed on a separate laptop.

**Figure 13.** The experimental set-up, showing the function generator, the smartphone tripod, and the blue mat where the subject received stimulation.

A side view of the experimental setup is shown in Figure 14. A meter stick was taped to the underside of a table. The alligator clips were taped to the edge of the meter stick over the pad. The thin platinum wires were allowed to freely hang from these alligator wires to minimize tension applied to the subjects when attached to the wires.
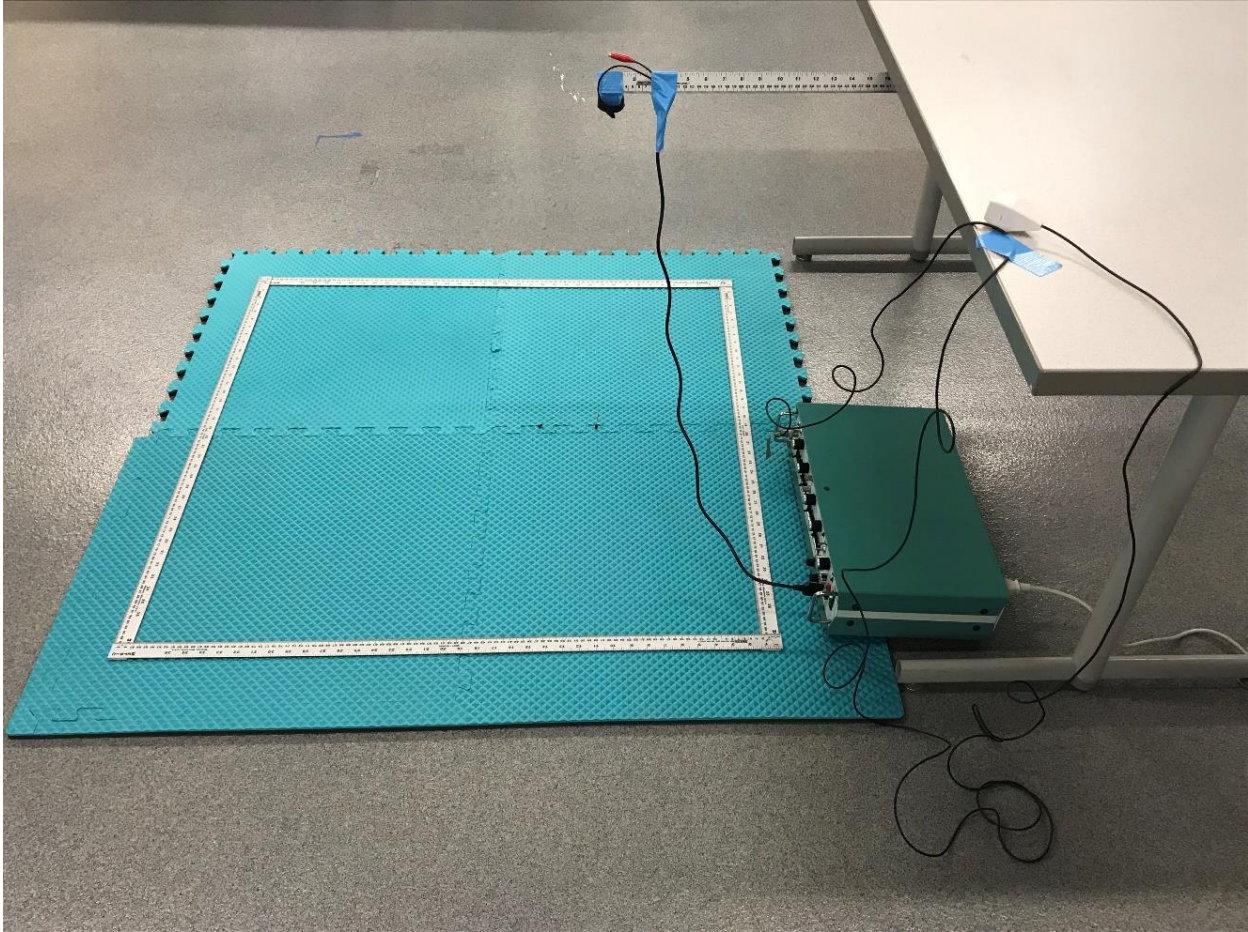
**Figure 14.** A side view of the experimental set-up, showing a meter stick holding thin platinum wires to ensure minimal tension was placed on the subjects.

Prior to beginning stimulation sessions with each subject, each subject was placed approximately in the center of the pad. The subjects would then be connected to the function generator as described in the previous section. After each stimulus and subsequent motion of the subject, the subject would be placed back in the approximate center of the pad.

### 3.6 Data Extraction from Video Files

Both custom MATLAB software and Kinovea software were used to extract motion data from the video files. Specific motion data extracted for each trial include horizontal and vertical coordinates, turn angles, angular velocities, and turn radii. Before extracting any motion data from each video in Kinovea, each video file was calibrated using the perspective grid function.

The grid was placed on the four corners of the meter sticks, as shown in Figure 15, and the size of the grid was set to 50 x 50 cm. This process ensured that measurements within the grid are accurate even if the plane of motion was not aligned with the smartphone camera [33].
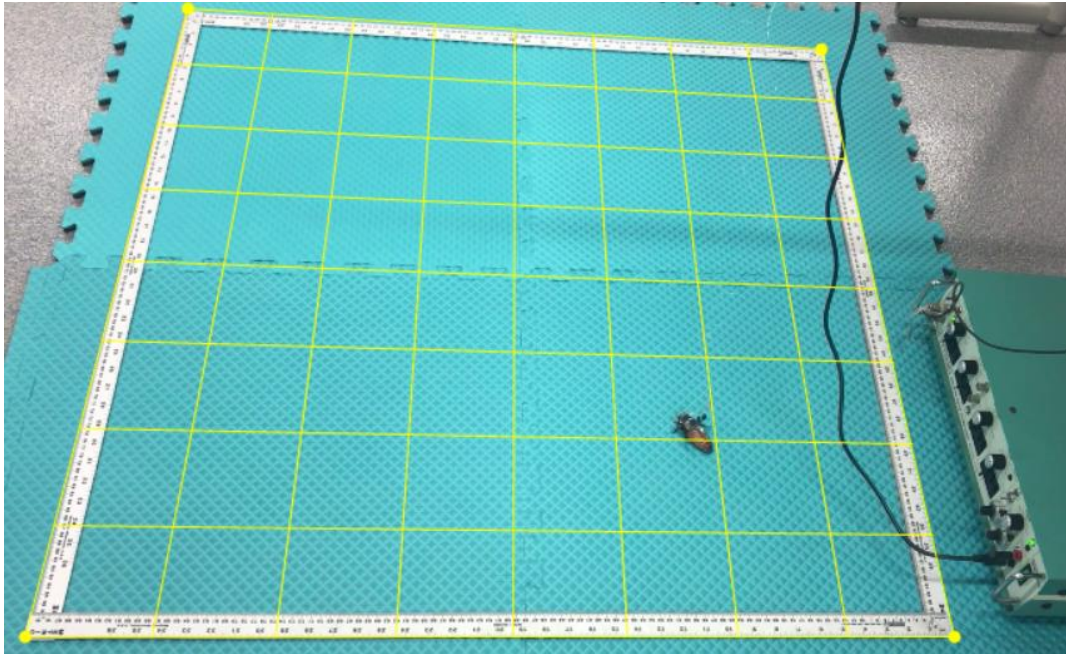


**Figure 15.** A grid placed on four corners of a square of meter sticks in a video file using Kinovea software, which ensures that measurements within the grid are accurate even if the plane of motion was not aligned with the smartphone camera.

To extract turn angles in Kinovea software, a line was drawn down the middle of the subject in each video at the beginning of the stimulus, which was indicated by the green light on the function generated. This step is shown in Figure 16. The angle function in Kinovea measured and tracked the angle between this line and the subject's head over time. An example of this function at a single time point is shown in Figure 17.
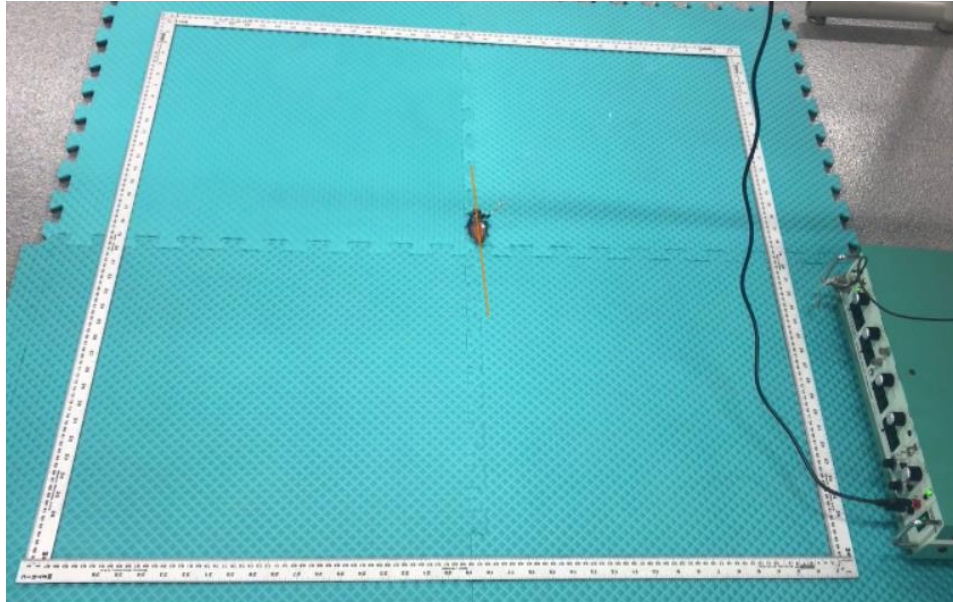
**Figure 16.** A line drawn down the middle of a subject in a video file using Kinovea software, which will be used in order to generate turn angle data.
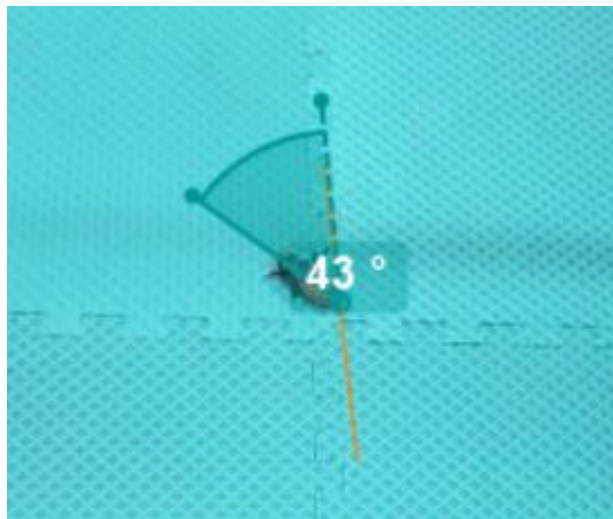


**Figure 17.** The angle function in Kinovea software was used to track and extract turn angle data from video files.

The turn angle data for each video file were then extracted to an excel file for further

processing.  An example of raw turn angle data over time is shown in Figure 18.
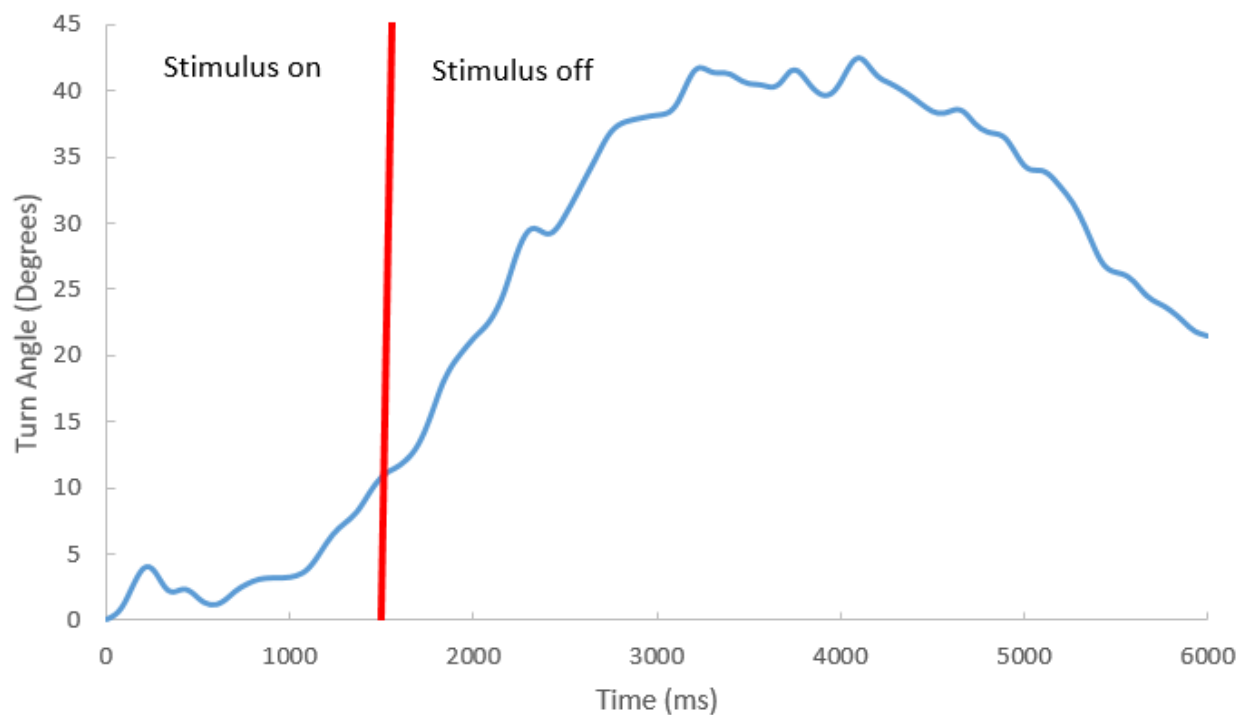
**Figure 18.** An example of cumulative turn angle data for 1 trial. This example is Subject 16's 8th trial, which used stimulus parameters of 1 V and 1.5 s.

3.7 Processing of Motion Data

Subjects 13, 17, and 18 were found to be completely unresponsive to electrical stimuli under any of the four sets of stimulus parameters. Accordingly, these subjects were excluded from any subsequent motion analysis, and all analyses found in the Results section were conducted using 17 subjects.

Response rates were computed for each subject under each set of stimulus parameters. A subject was deemed "responsive" during a given trial if the subject turned greater than 5° in any direction during or in the 6 seconds after a stimulus was applied.

Subjects often exhibited a 2-phase turning response, where they would initially turn in the contralateral direction as the stimulus followed by a "corrective" turn where they would turn in the ipsilateral direction of the stimulus. An example of this 2-phase turning response is seen

above in Figure 18.  In further processing of motion data, the initial turn is denoted as a primary

turn, and the "corrective" turn is denoted as a secondary turn.  In order to determine an adequate

and consistent method to separate cumulative turn angles into primary and secondary turn angles,

the average time of maximum cumulative turn angle for trials that exhibited a 2-phase turning

response was computed for each subject under all four sets of stimulus parameters.  The average

time of maximum cumulative turn angle for all trials that exhibited a 2-phase turning response

for each subject was similar under all four sets of stimulus parameters at approximately 2

seconds after completion of stimulation.  For instance, Figure 18 above shows the maximum

cumulative turn angle at approximately 3500 milliseconds, which is approximately 2 seconds

after the stimulation duration of 1500 milliseconds. Therefore, the primary turn was denoted as

the turning behavior from the completion of stimulation to 2 seconds after the completion of

stimulation.  Eq. 1 below shows an example of a primary turn angle calculation using the data

found in Figure 18, where Turn $Angle_2$ is equal to the cumulative turn angle 2 seconds after

completion of stimulation and Turn $Angle_1$ is equal to the cumulative turn angle at the

completion of stimulation.

$$(1)\ Cumulative\ Primary\ Turn\ Angle = \ Turn\ Angle_2 - Turn\ Angle_1 = 40.55 - 10.78 = 29.77\ degrees$$

Accordingly, the secondary turn was defined as the turning behavior from 2 seconds after

the completion of stimulation to 4.5 seconds after the completion of stimulation.  4.5 seconds

was after stimulation was chosen in order to keep the secondary turn in the 6-second range in

which turn angle data was collected for this research.  Eq.2 below shows an example of a

secondary turn angle calculation, again using data found in Figure 18.  Turn $Angle_3$ is equal to

the cumulative turn angle 4.5 seconds after completion of stimulation.

$$(2)\ Cumulative\ Secondary\ Turn\ Angle = \ Turn\ Angle_3 - Turn\ Angle_2 = 21.45 - 40.55 = -19.1\ degrees$$

3.8 Statistical Analyses

3.8.1 Response Rates

In order to determine if response rates to antennal stimulation were dependent on the voltage, duration, or interaction of voltage and duration of the pulse stimulus, a linear regression analysis was conducted. P-values corresponding to the voltage, duration, and interaction of the two factors were computed using $p < 0.05$ to indicate statistical significance.

3.8.2 Primary and Secondary Turn Rates in the Contralateral Direction

Primary turn angles were calculated by subtracting the cumulative turn angle at the completion of stimulation from the cumulative turn angle two seconds after the stimulation ended. If the primary turn angle was positive, it was deemed a turn in the contralateral direction. Rates that primary turns were in the contralateral direction were computed for each subject under each set of stimulus parameter.

In order to determine if primary turn rates in the contralateral direction to antennal stimulation were dependent on the voltage, duration, or interaction of voltage and duration of the pulse stimulus, a linear regression analysis was conducted. P-values corresponding to the voltage, duration, and interaction of the two factors were computed using $p < 0.05$ to indicate statistical significance.

Individual subject primary turn rates in the contralateral direction to stimulation were analyzed to determine the percentage of subjects that antennal stimulation significantly induced primary turns in the intended direction. If "chance" was the only factor affecting turn rate in the contralateral direction, it would be expected that the turn rate in the contralateral direction would be approximately 50%. Therefore, 1-proportion t-tests were conducted for each subject under

each set of stimulus parameters to determine if the primary turn rate in the contralateral direction was significantly higher than 50% using $p < 0.05$ to indicate statistical significance.

Secondary turns were calculated by subtracting the turn angle 2 seconds after completion of stimulation from the turn angle 4.5 seconds after completion of stimulation. If the secondary angle was positive, it was deemed a turn in the contralateral direction. Rates that secondary turns were in the contralateral direction were computed for each subject under each set of stimulus parameter.

Similarly to the analyses on primary turn rates in the contralateral direction, to determine if secondary turn rates in the contralateral direction to antennal stimulation were dependent on the voltage, duration, or interaction of voltage and duration of the pulse stimulus, a linear regression analysis was conducted. Again, p-values corresponding to the voltage, duration, and interaction of the 2 factors were computed using $p < 0.05$ to indicate statistical significance.

Individual subject secondary turn rates in the contralateral direction to stimulation were also analyzed to determine the percentage of subjects that antennal stimulation significantly induced secondary turns in the intended direction. 1-proportion t-tests were conducted for each subject under each set of stimulus parameters to determine if the secondary turn rate in the contralateral direction was significantly different than 50% using $p < 0.05$ to indicate statistical significance.

### 3.8.3 Primary and Secondary Turn Magnitudes

In order to determine if the voltage, duration, or interaction of voltage and duration of the stimulus affected the primary turn magnitude, a linear regression analysis was conducted.  P-values corresponding to the voltage, duration, and interaction of the 2 factors were computed using $p < 0.05$ to indicate statistical significance.  Similarly, a linear regression analysis was conducted in order to determine if the voltage, duration, or interaction of voltage and duration of the stimulus affected the secondary turn magnitude.

# 4. RESULTS

### 4.1 Response Rates

For all subjects that were responsive to any antennal stimulation (n=17), individual subject's response rates were calculated for the four sets of stimulus parameters. A subject was deemed responsive for the respective trial if the specimen turned at least 5° in either direction in the six seconds during and following stimulation. Histograms showing the frequency of response rates for each set of stimulus parameter is shown in Figure 19. The average response rates and individual standard deviations for each set of stimulus parameters were similar. The highest average response rate achieved was 87.06 ±12.94% using a stimulus voltage of 3 V and a duration of 1.5 s, while the lowest average response rate achieved was 85.02 ± 14.98% using a stimulus voltage of 1 V and a duration of 1.5 s.
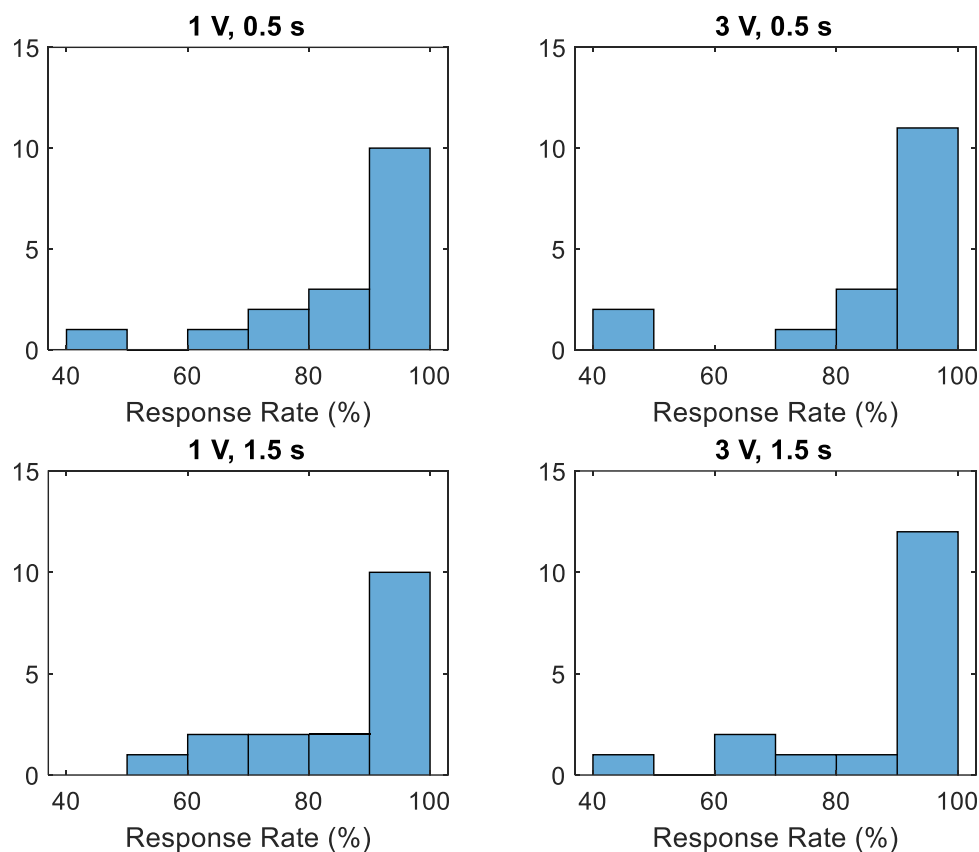
**Figure 19.** Histogram of response rates to antennal stimulation under different stimulus parameters for all subjects (n=17). The frequencies of response rates for each set of stimulus parameters are very similar, demonstrating that there was not a significant difference in response rate based on voltage or duration of the stimulus.

A linear regression analysis was used to determine if the voltage of the stimulus, duration of the stimulus, or the interaction of voltage and duration affected response rates. P-values corresponding to the stimulus voltage, duration, and interaction of the 2 factors were found to be 0.971, 0.878, and 0.802, respectively. These high p-values ($p > 0.05$) demonstrate that there is not a statistically significant difference in response rates based on stimulus voltage, duration, or the interaction of the 2 parameters.

4.2 Turn Angle Analysis Overview

In most subjects, the majority of trials resulted in cumulative turns in the contralateral direction of stimulation. High intrasubject variability was exhibited in all subjects. Often, subjects initially turned in the contralateral direction (denoted as primary turn), followed by a corrective turn in the ipsilateral direction (denoted as secondary turn). During stimulation, most subjects "cringed" and did not move; in this case, subjects would begin turning shortly after stimulation ended. However, a few subjects would begin turning upon the start of stimulation and did not exhibit this "cringe" behavior. An illustrative example of the turn angle analysis for one subject receiving four sets of stimulus parameters is shown in Figure 20, with a turn in the contralateral direction shown as a positive turn angle. As seen in Figure 20, the majority of trials resulted in relatively low cumulative turn angles during the stimulation period; this is representative of the subject's "cringe" response before its primary turn. Cumulative turn angle data was processed as described in Section 3.7 and used in further analyses in the following sections. Cumulative turn angle data for all subjects can be found in Appendix B.
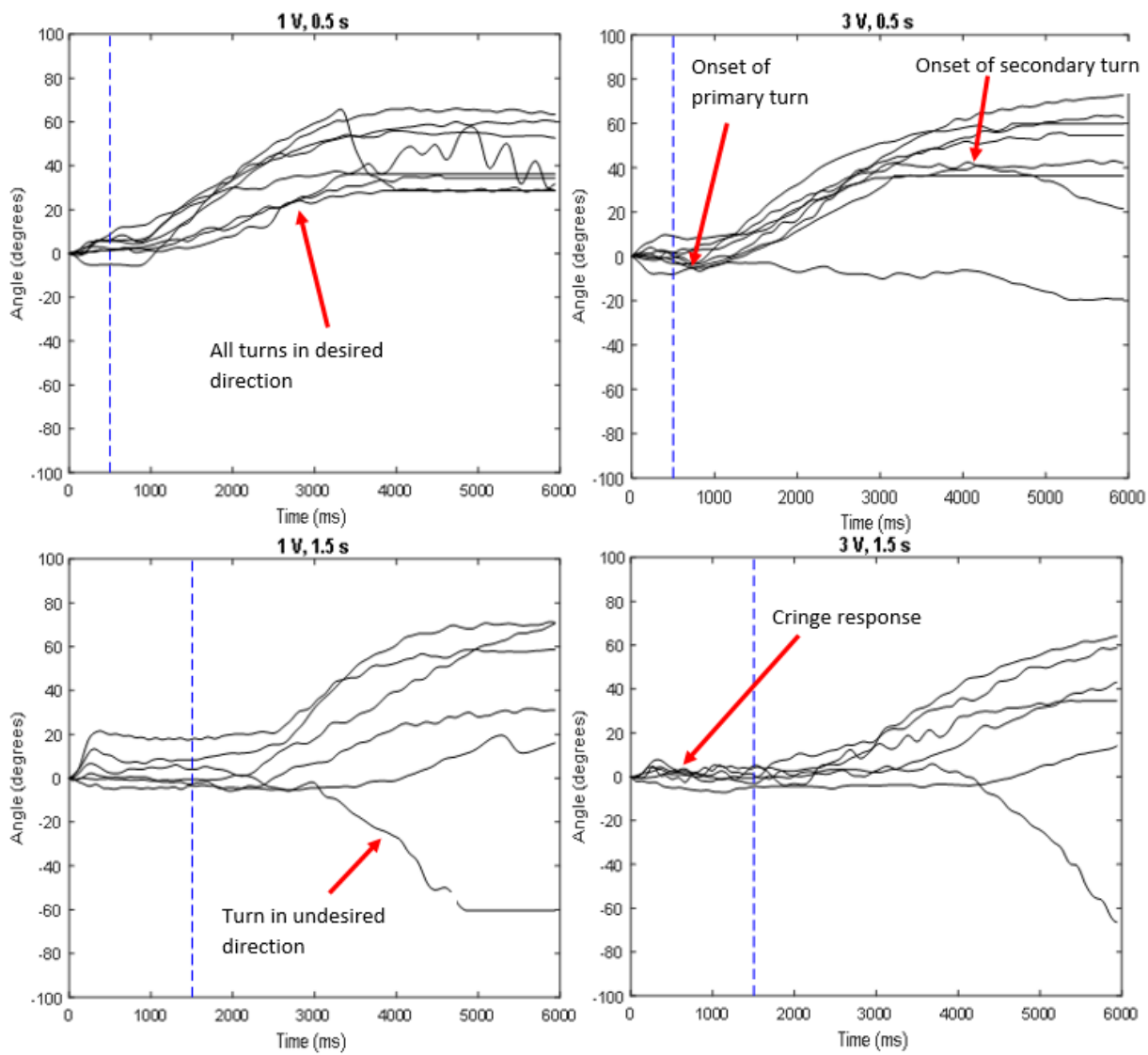
**Figure 20.** Cumulative turn angle data for Subject 16 following stimulation with four different sets of stimulus parameters. Positive turn angles correspond with the contralateral direction of stimulation. The dashed blue lines indicates the completion of stimulation.

4.3 Primary Turn Response

Most subjects initiated turning in the contralateral direction shortly after the stimulation ended.  Primary turn angles were calculated by subtracting the cumulative turn angle at the completion of stimulation from the cumulative turn angle two seconds after the stimulation ended.  If the primary turn angle was positive, it was deemed a turn in the contralateral direction. Histograms showing the frequency of percentages of primary turns in the contralateral direction for each set of stimulus parameters are shown in Figure 21, demonstrating that 100% rates of turns in the contralateral direction can be achieved by most subjects under the stimulation parameters of 3 V, 0.5 s.
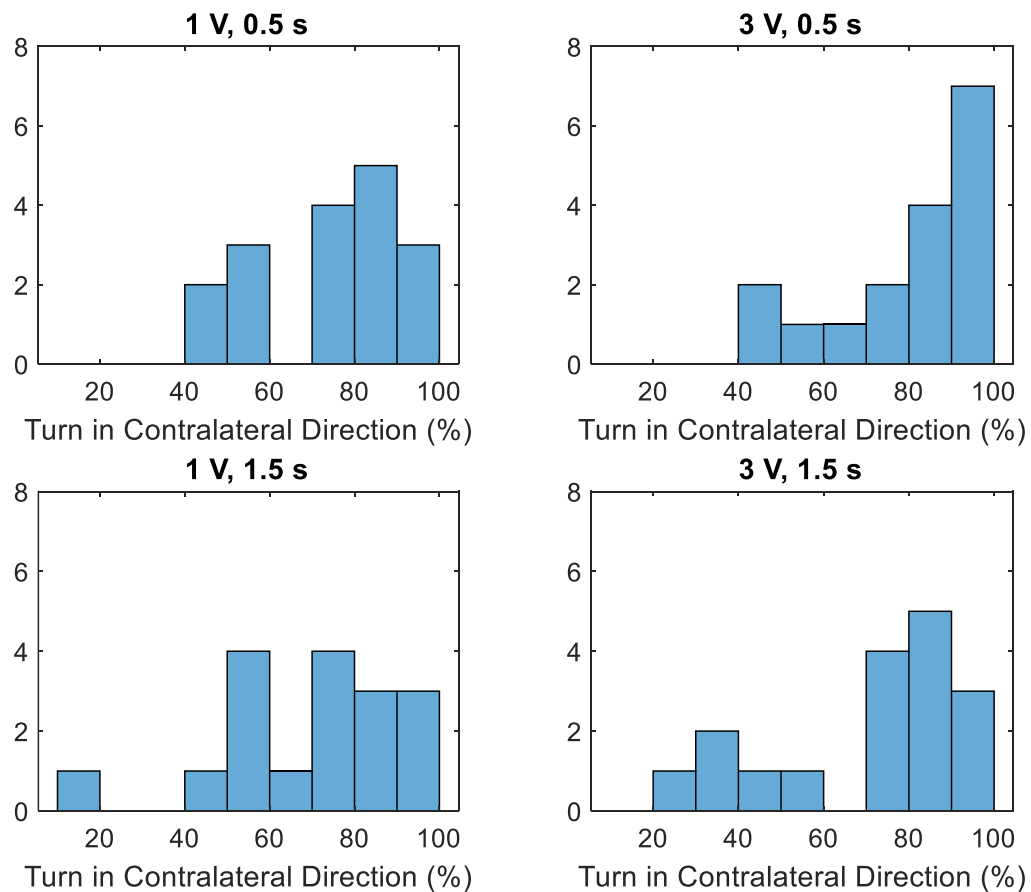


**Figure 21.** Histogram of primary turn rates in the contralateral direction in response to antennal stimulation under different stimulus parameters for all subjects (n=17).  3 V and 0.5 s demonstrates the highest rates of primary turns in the contralateral direction.

A linear regression analysis was used to determine if the voltage of the stimulus, duration of the stimulus, or the interaction of voltage and duration affected percentages of primary turns in the contralateral direction. P-values corresponding to the stimulus voltage, duration, and interaction of the two factors were found to be 0.458, 0.795, and 0.656, respectively. These high p-values ($p > 0.05$) demonstrate that there is not a statistically significant difference in rates of primary turns in the contralateral direction based on stimulus voltage, duration, or the interaction of the two parameters.

While all subjects included in the following analysis were responsive to electrical stimulation, some subjects were not predictable in the direction of their subsequent primary turn. Therefore, individual subjects were analyzed to determine if the antennal stimulation did significantly induce primary turns in the contralateral direction. As an illustration, Figure 22 shows the percentage of initial turns, or primary turns, that were in the contralateral direction for Subject 16. The dashed line shows the percentage of primary turns that would be expected in the contralateral direction due to only chance. As Figure 22 shows, all four sets of stimulus parameters had percentages of primary turns in the contralateral direction that was higher than chance.
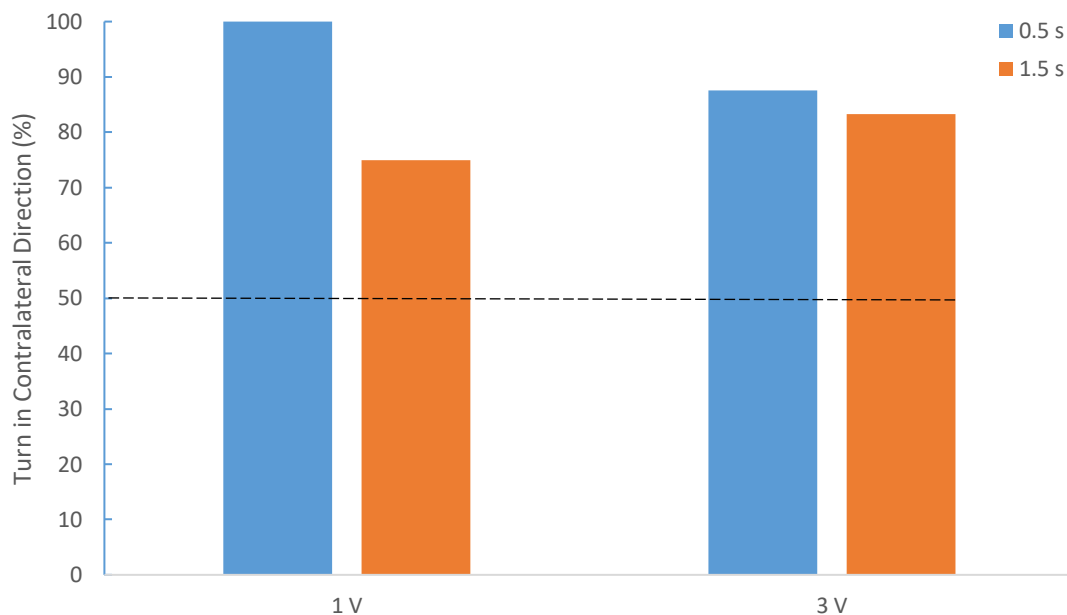
**Figure 22.** The percentages that Subject 16's primary turn was in the contralateral direction of stimulation under different stimulus parameters. The primary turn angle was calculated by subtracting the turn angle at the end of stimulation from the turn angle 2 seconds after stimulation completion. The dashed line indicates the percentage of primary turns that would be expected in the contralateral direction due to only chance.

1-proportion t-tests were conducted on for each set of stimulus parameters to determine if the difference between the percentage of primary turns in the contralateral direction and the expected percentage due to chance (50%) was statistically significant. The results of these 1-proportion t-tests for Subject 16 are shown in Table 3.

**Table 3.** P-values for 1-proportion t-tests to determine if there is a statistically significant difference between the percentage of primary turns in the contralateral direction and the expected percentage due to chance for each set of stimulus parameters for Subject 16.

|         | 1 V, 0.5 s | 3 V, 0.5 s | 1 V, 1.5 s | 3 V, 1.5 s |
|---------|------------|------------|------------|------------|
| p-value | 0.001      | 0.035      | 0.144      | 0.109      |

Table 4 contains the percentages of primary turns in the contralateral directions under all stimulus parameter groups and for all subjects, as well as the p-values associated with 1-proportion t-tests. Approximately 88% of subjects had at least one set of stimulus parameters in which there was a statistically significant difference between the percentage of primary turns in

the contralateral direction and the expected percentage due to chance. A voltage of 3 V and duration of 0.5 s was found to have the highest percentages of primary turns in the contralateral direction, with approximately 65% of subjects having statistically significant differences between the percentage of primary turns in the contralateral direction and expected percentage due to chance.

**Table 4.** For all subjects, the percentages of primary turns in the contralateral direction under all four sets of stimulus parameters. The p-values associated with 1-proportion t-tests, which were used to determine if there was a statistically significant difference between the percentage of primary turns in the contralateral direction and the expected percentage due to change (50%), are also included.

| Subject | 1 V, 0. 5 s | | 3 V, 0.5 s | | 1 V, 1.5 s | | 3 V, 1.5 s | |
|---|---|---|---|---|---|---|---|---|
| | % Turn in Contralateral Direction | p-value | % Turn in Contralateral Direction | p-value | % Turn in Contralateral Direction | p-value | % Turn in Contralateral Direction | p-value |
| 1 | 50 | 0.623 | 77.77 | 0.090 | 55.55 | 0.500 | 75 | 0.144 |
| 2 | 75 | 0.144 | 40 | 0.828 | 100 | 0.001 | 88.88 | 0.019 |
| 3 | 50 | 0.623 | 90 | 0.011 | 62.5 | 0.363 | 90 | 0.011 |
| 4 | 100 | 0.001 | 50 | 0.623 | 42.85 | 0.773 | 33.33 | 0.910 |
| 5 | 71.43 | 0.226 | 60 | 0.377 | 57.14 | 0.500 | 85.71 | 0.063 |
| 6 | 90 | 0.011 | 100 | 0.001 | 100 | 0.001 | 90 | 0.011 |
| 7 | 55.55 | 0.500 | 90 | 0.011 | 80 | 0.055 | 88.88 | 0.019 |
| 8 | 83.33 | 0.109 | 85.71 | 0.063 | 50 | 0.623 | 44.44 | 0.746 |
| 9 | 87.50 | 0.035 | 100 | 0.001 | 71.43 | 0.227 | 50 | 0.623 |
| 10 | 87.5 | 0.035 | 80 | 0.055 | 75 | 0.144 | 77.77 | 0.090 |
| 11 | 44.44 | 0.746 | 44.44 | 0.746 | 11.11 | 0.998 | 37.50 | 0.855 |
| 12 | 75 | 0.144 | 100 | 0.001 | 87.5 | 0.035 | 25 | 0.965 |
| 13 | N/A | N/A | N/A | N/A | N/A | N/A | N/A | N/A |
| 14 | 40 | 0.828 | 100 | 0.001 | 50 | 0.623 | 75 | 0.144 |
| 15 | 88.88 | 0.019 | 90 | 0.011 | 70 | 0.172 | 77.77 | 0.090 |
| 16 | 100 | 0.001 | 87.5 | 0.035 | 75 | 0.144 | 83.33 | 0.109 |
| 17 | N/A | N/A | N/A | N/A | N/A | N/A | N/A | N/A |
| 18 | N/A | N/A | N/A | N/A | N/A | N/A | N/A | N/A |
| 19 | 88.88 | 0.019 | 77.77 | 0.090 | 88.88 | 0.019 | 80 | 0.055 |
| 20 | 70 | 0.172 | 80 | 0.055 | 100 | 0.001 | 100 | 0.001 |

The magnitude of primary turns for each subject was also computed. Figure 23 shows the histogram of average primary turn magnitudes for all subjects (n=17). A voltage of 1 V and duration of 0.5 s resulted in the highest mean magnitude of primary turn of $15.20 \pm 9.88$ degrees, while a voltage of 3 V and duration of 1.5 s resulted in the lowest mean magnitude of primary

turn of 7.79 ± 11.46 degrees. However, a voltage of 3 V and duration of 0.5 s resulted in the most consistent control of the subjects, with only one subject being outside the primary turn angle range of 0°-30°.
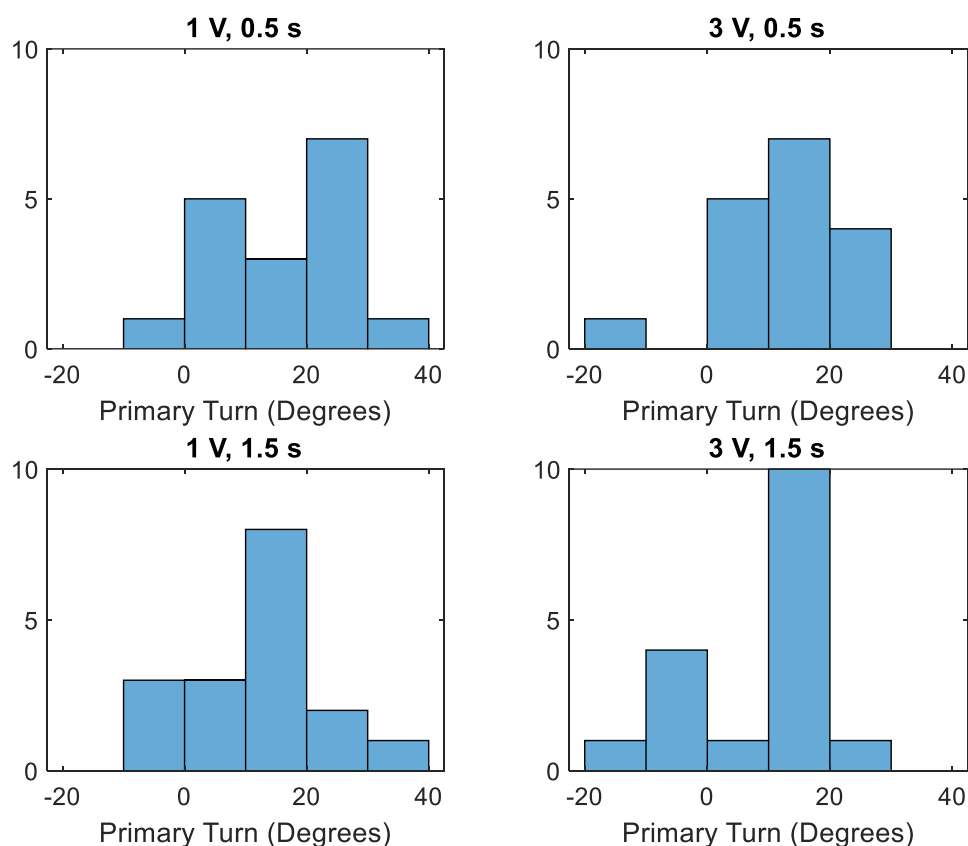


**Figure 23.** Histogram of average primary turn magnitudes in response to antennal stimulation under different stimulus parameters for all subjects (n=17).

In order to determine if the voltage, duration, or interaction of the two factors have an effect on primary turn magnitude, a linear regression analysis was conducted. P-values corresponding to the stimulus voltage, duration, and interaction of the two factors were found to be 0.812, 0.586, and 0.714, respectively. These high p-values ($p>0.05$) demonstrate that there is not a statistically significant difference in magnitudes of primary turns based on stimulus voltage, duration, or the interaction of the two parameters.

High intrasubject variability in magnitudes of primary turns were observed in most subjects. Figure 24 is exemplary of this high variability; Figure 24 shows the median magnitudes and $25^{th}$ and $75^{th}$ percentiles of primary turns for each set of stimulus parameters for Subject 16.
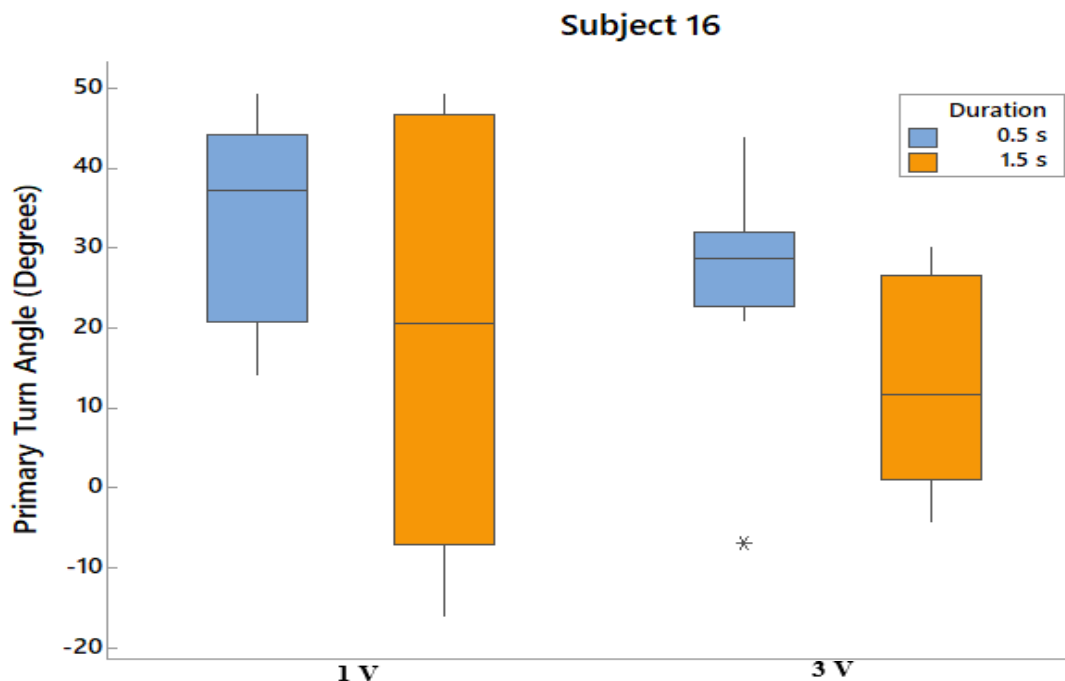


**Figure 24.** Primary turn angles for Subject 16 under differing stimulus parameters. The primary turn angle was calculated by subtracting the turn angle at the end of stimulation from the turn angle 2 seconds after stimulation completion.

4.4 Secondary Turn Response

Subjects sometimes exhibited a "corrective" turn, where they would turn in the same direction of the stimulation location after about 2 seconds - 3.5 seconds after the completion of stimulation. Therefore, secondary turns were calculated by subtracting the cumulative turn angle 2 seconds after completion of stimulation from the turn angle 4.5 seconds after completion of stimulation. If the secondary angle was positive, it was deemed a turn in the contralateral direction. Histograms showing the percentages of secondary turn rates in the contralateral direction for each set of stimulus parameters are shown in Figure 25. A voltage of 3 V and

duration of 0.5 s produced the most subjects with high percentages of secondary turns in the

contralateral direction.  Furthermore, 3 V and 0.5 s had a less variable spread of percentages of
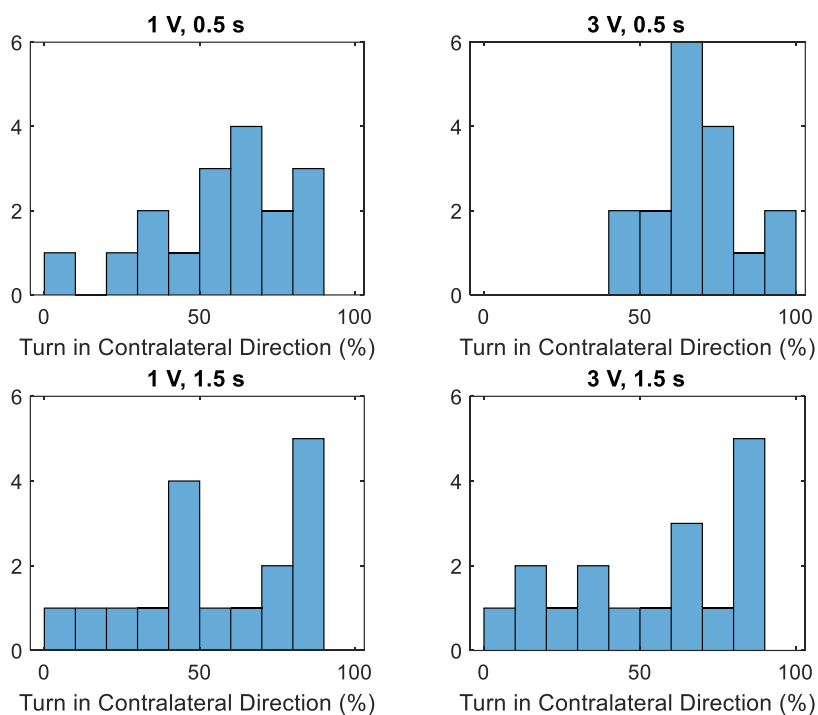
secondary turns in the contralateral direction.



**Figure 25.** Histogram of secondary turn rates in the contralateral direction in response to antennal stimulation under different stimulus parameters for all subjects (n=17).  3 V and 0.5 s demonstrates the highest rates of secondary turns in the contralateral direction.

A linear regression analysis was used to determine if the voltage of the stimulus, duration

of the stimulus, or the interaction of voltage and duration affected the percentages of secondary

turns in the contralateral direction.  P-values corresponding to the stimulus voltage, duration, and

interaction of the two factors were found to be 0.138, 0.645, and 0.220, respectively.  These high

p-values (p>0.05) demonstrate that there is not a statistically significant difference in percentages

of secondary turns in the contralateral direction based on stimulus voltage, duration, or the

interaction of the two parameters.

Individual subjects secondary turn data were analyzed to determine if the antennal stimulation significantly induced secondary turns in either direction. Figure 26 shows the percentage of secondary turns that were in the contralateral direction for Subject 16. The dashed line shows the percentage of secondary turns that would be expected in the contralateral direction due to only chance. For Subject 16, the rates of secondary turns in the contralateral direction was less than the rates of primary turns in the contralateral direction.
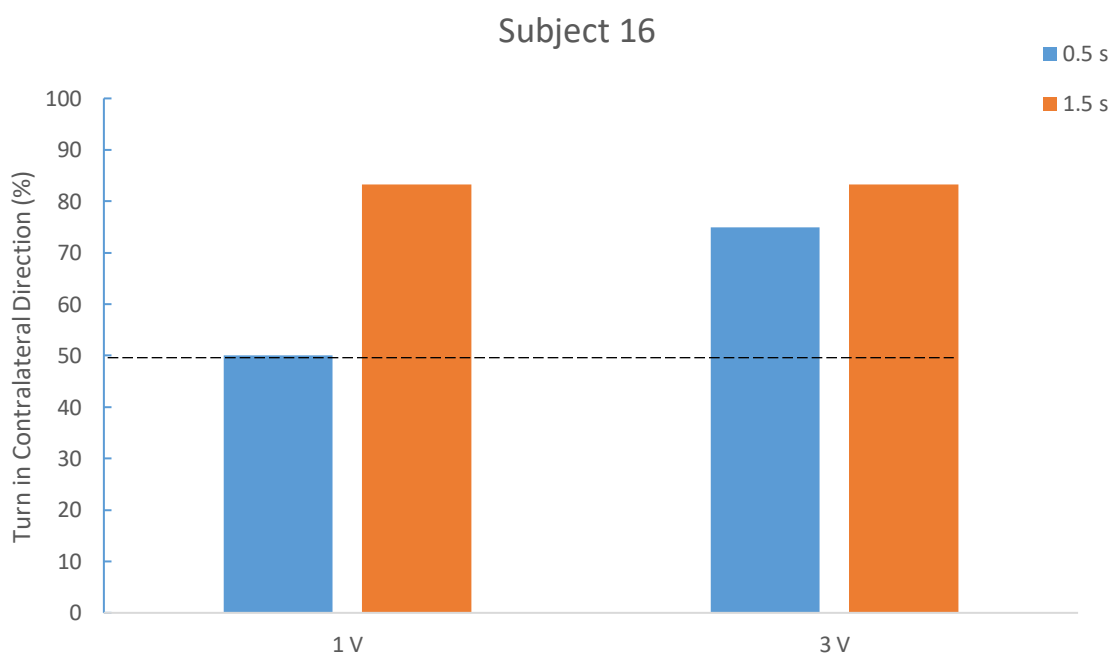


**Figure 26.** The percentages that Subject 16's secondary turn was in the contralateral direction of stimulation under different stimulus parameters. The secondary turn angle was calculated by subtracting the turn angle 2 seconds after stimulation from the turn angle 4.5 seconds after stimulation. The dashed line indicates the percentage of secondary turns that would be expected in the contralateral direction due to only chance.

1-proportion t-tests were conducted for each set of stimulus parameters to determine if the difference between the percentage of secondary turns in the contralateral direction and the expected percentage due to chance (50%) was statistically significant. The results of these 1-proportion t-tests for Subject 16 are shown in Table 5.

**Table 5.** P-values for 1-proportion t-tests to determine if there is a statistically significant difference between the percentage of secondary turns in the contralateral direction and the expected percentage due to chance for each set of stimulus parameters for Subject 16.

| | 1 V, 0.5 s | 3 V, 0.5 s | 1 V, 1.5 s | 3 V, 1.5 s |
|---|---|---|---|---|
| p-value | 0.623 | 0.144 | 0.109 | 0.109 |

Table 6 contains the percentages of secondary turns in the contralateral direction under all parameters for all subjects, as well as the 1-proportion t-tests' corresponding p-values. Approximately 52.94% of subjects had at least 1 set of stimulus parameters in which there was a statistically significant difference between the percentage of secondary turns in the contralateral direction and the expected percentage due to chance. A voltage of 1 V and duration of 1.5 s as well as 3 V and 1.5 s were found to have the highest percentages of secondary turns in the contralateral direction, with approximately 29.41% of subjects having statistically significant differences between the percentage of secondary turns in the contralateral direction and expected percentage due to chance.

**Table 6.** For all subjects, the percentages of secondary turns in the contralateral direction under all four sets of stimulus parameters. The p-values associated with 1-proportion t-tests, which were used to determine if there was a statistically significant difference between the percentage of secondary turns in the contralateral direction and the expected percentage due to change (50%), are also included.

| Subject | 1 V, 0.5 s % Turn in Contralateral Direction | p-value | 3 V, 0.5 s % Turn in Contralateral Direction | p-value | 1 V, 1.5 s % Turn in Contralateral Direction | p-value | 3 V, 1.5 s % Turn in Contralateral Direction | p-value |
|---|---|---|---|---|---|---|---|---|
| 1 | 62.50 | 0.363 | 55.55 | 0.5 | 44.44 | 0.746 | 62.50 | 0.363 |
| 2 | 87.50 | 0.035 | 60 | 0.377 | 55.55 | 0.5 | 33.33 | 0.910 |
| 3 | 80 | 0.055 | 70 | 0.172 | 37.5 | 0.855 | 70 | 0.172 |
| 4 | 50 | 0.623 | 50 | 0.623 | 42.86 | 0.773 | 16.66 | 0.984 |
| 5 | 57.14 | 0.500 | 60 | 0.377 | 85.71 | 0.062 | 42.86 | 0.773 |
| 6 | 70 | 0.172 | 66.66 | 0.254 | 87.50 | 0.035 | 80 | 0.055 |
| 7 | 44.44 | 0.746 | 60 | 0.377 | 60 | 0.377 | 88.88 | 0.019 |
| 8 | 33.33 | 0.910 | 85.71 | 0.062 | 40 | 0.828 | 22.22 | 0.980 |
| 9 | 25 | 0.965 | 66.66 | 0.254 | 14.29 | 0.992 | 66.66 | 0.254 |
| 10 | 37.5 | 0.855 | 40 | 0.828 | 87.5 | 0.035 | 55.55 | 0.500 |
| 11 | 0 | 0.999 | 44.44 | 0.746 | 0 | 0.999 | 12.5 | 0.996 |

| 12 | 75 | 0.144 | 100 | 0.001 | 25 | 0.965 | 0 | 0.999 |
| 13 | N/A | N/A | N/A | N/A | N/A | N/A | N/A | N/A |
| 14 | 60 | 0.377 | 75 | 0.144 | 80 | 0.055 | 62.50 | 0.363 |
| 15 | 90 | 0.011 | 90 | 0.011 | 70 | 0.172 | 33.33 | 0.910 |
| 16 | 50 | 0.623 | 75 | 0.144 | 83.33 | 0.109 | 83.33 | 0.109 |
| 17 | N/A | N/A | N/A | N/A | N/A | N/A | N/A | N/A |
| 18 | N/A | N/A | N/A | N/A | N/A | N/A | N/A | N/A |
| 19 | 66.66 | 0.254 | 77.77 | 0.090 | 44.44 | 0.746 | 80 | 0.055 |
| 20 | 60 | 0.377 | 60 | 0.377 | 72.72 | 0.113 | 88.88 | 0.019 |

The magnitude of secondary turns for each subject was also computed. Figure 27 shows the frequency of average secondary turn magnitudes for all subjects (n=17). A voltage of 3 V and duration of 0.5 s resulted in the highest mean magnitude of primary turn of $11.06 \pm 16.49$ degrees, while a voltage of 3 V and duration of 1.5 s resulted in the lowest mean magnitude of primary turn of $0.05 \pm 8.02$ degrees.
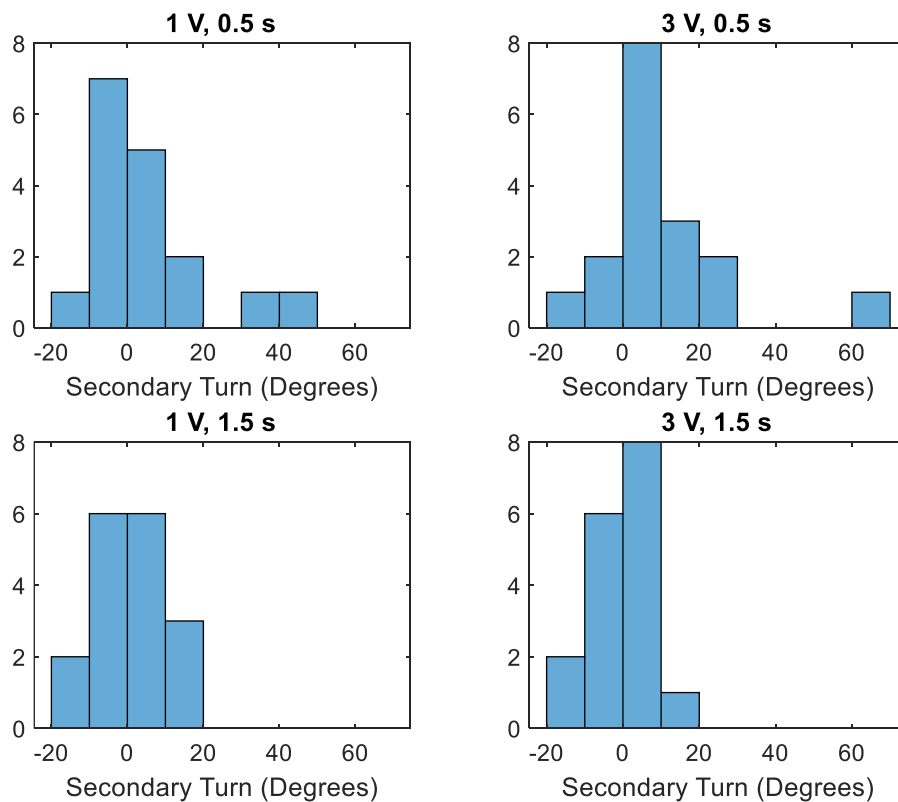


**Figure 27.** Histogram of average secondary turn magnitudes in response to antennal stimulation under different stimulus parameters for all subjects (n=17).

To determine if the voltage, duration, or interaction of the two factors have an effect on secondary turn magnitude, a linear regression analysis was conducted. P-values corresponding to the stimulus voltage, duration, and interaction of the two factors were found to be 0.174, 0.790, and 0.265, respectively. These high p-values ($p>0.05$) demonstrate that there is not a statistically significant difference in magnitudes of secondary turns based on stimulus voltage, duration, or the interaction of the two parameters.

Similar to primary turns, high intrasubject variability in magnitudes of secondary turns were observed in most subjects. Figure 28 is exemplary of this high variability; Figure 28 shows the median magnitudes and 25th and 75th percentiles of secondary turns for each set of stimulus parameters for Subject 16. As displayed, stimuli with a voltage of 3 V and a duration of 1.5 s resulted in the highest median secondary turn angle for this subject.
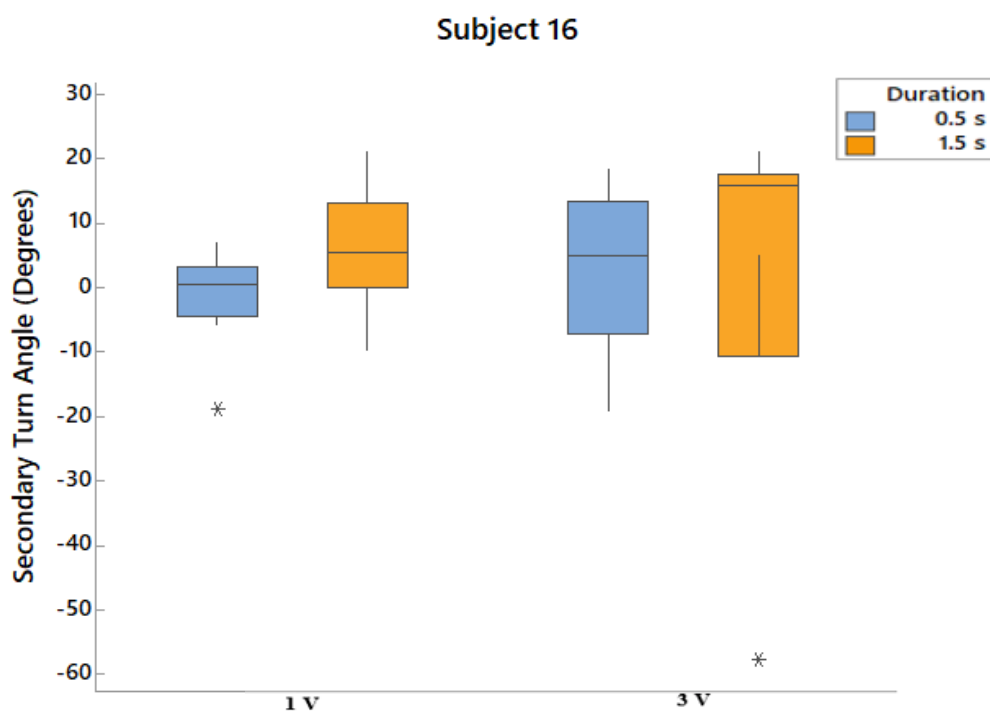


**Figure 28.** Secondary turn angles for Subject 16 under differing stimulus parameters. The secondary turn angle was calculated by subtracting the turn angle 2 seconds after stimulation from the turn angle 4.5 seconds after stimulation.

4.5 Habituation Response

A slight decrease in primary turn magnitudes was observed over time for most subjects. Figure 29 shows the magnitude of primary turns versus the trial number for Subject 16. Despite the high variability in primary turn magnitude, the dashed line demonstrates a slight decrease over time.
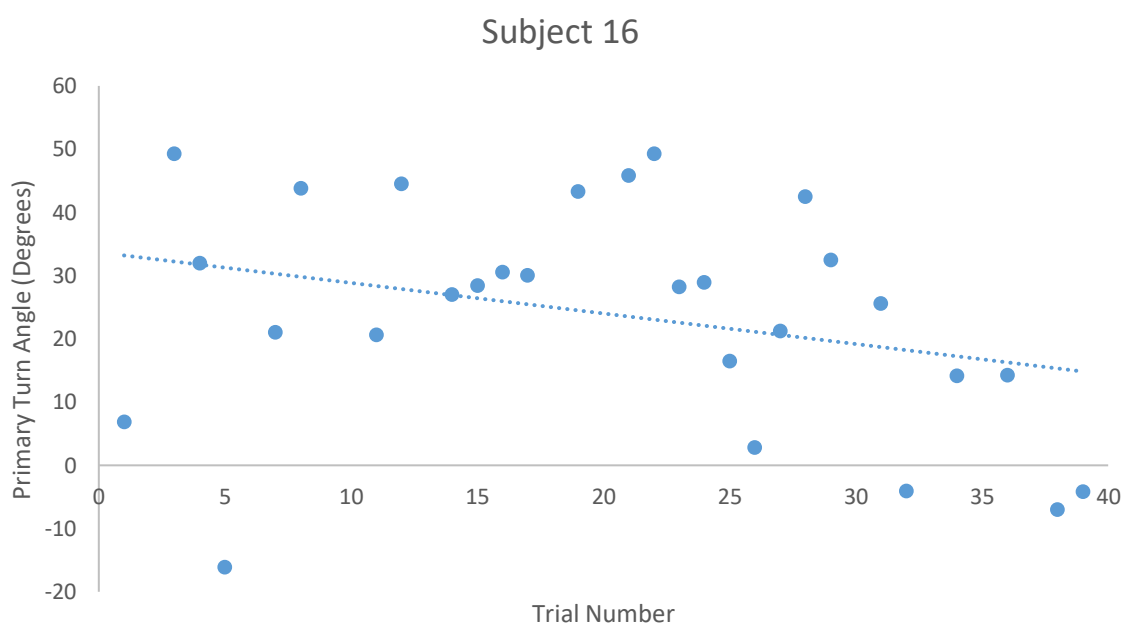


**Figure 29.** Primary turn magnitudes over time for Subject 16. The dashed line indicates a linear fit, demonstrating a slight decrease in primary turn magnitude over time.

Despite the slight decrease in primary turn magnitudes over time, this effect was not observed in secondary turn magnitudes. Figure 30 below shows the magnitude of secondary turns versus the trial number for Subject 16. The dashed line indicates that there is no significant increase or decrease in secondary turn angle magnitudes over time.
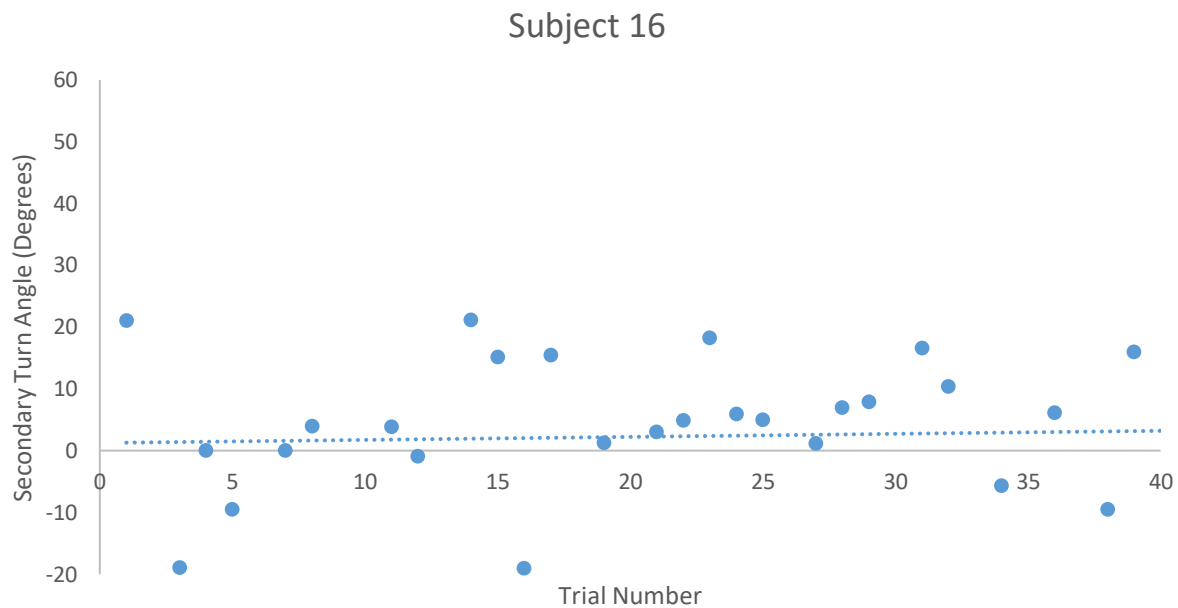
**Figure 30.** Secondary turn angle magnitudes over time for Subject 16. The dashed line indicates a linear fit, demonstrating approximately no increase or decrease in secondary turn magnitude over time.

**5. DISCUSSION**

The primary goal of this research was to improve the MHC biobot technology to the point it could be fully implemented commercially.  One way to improve the MHC biobot technology is to improve the response rates.  However, response rates were not found to be dependent on the stimulus voltage, stimulus duration, or the interaction of the voltage and duration in any of the given voltage and duration ranges tested.  Responses rates do appear to be subject dependent, with some subjects associated with very high response rates across all ranges of stimulus voltages and durations tested.  In further studies, initial evaluations should be used to identify subjects that consistently demonstrate high response rates; then, subsequent testing should include only this subset of subjects.  This will ensure that only subjects that are highly responsive to antennal stimulation are utilized, which would ultimately improve the reliability of MHC biobots.

Three subjects were completely unresponsive to stimulation under any of the stimulus parameters tested.  One possible explanation for the few subjects' complete unresponsiveness is variability in the anatomy of the subjects.  For instance, MHCs often break antennae living in captivity.  The MHCs are able to survive without antennae, demonstrating that the neural pathways in the antennae are not critical for survival.  It is possible that the unresponsive subjects had malfunctioning neurons in the antennae, but the antennae were still physically intact.  Incorrect electrode placement in the antennae, while possible, is an unlikely explanation as these subjects were unresponsive to stimulation in both antennae.

In order to direct motion of MHC biobots, the antenna contralateral to the desired direction was stimulated.  The average percentages of primary turns in the contralateral direction was measured, but these were not found to be dependent upon amplitude, pulse duration, or the

interaction of amplitude and duration. The average percentages of secondary turns in the contralateral direction were also not found to be dependent upon amplitude, pulse duration, or the interaction of amplitude and duration. However, an amplitude of 3 V was associated with slightly higher (p = 0.138) percentages of secondary turns in the contralateral direction. As shown in Figure 25, an amplitude of 3 V and duration of 0.5 s were also found to have the highest percentage of primary turns in the contralateral direction. Therefore, to direct MHC biobots in the desired direction for longer and reduce the magnitude of a "corrective" turn, stimuli with an amplitude of 3 V, duration of 0.5 s, frequency of 125 Hz, and duty cycle of 50% are deemed effective.

Approximately 88% of subjects had at least 1 set of stimulus parameters that could significantly control the direction of the primary turn, while only 53% of subjects had at least 1 set of stimulus parameters that could significantly control the direction of the secondary turn. Additionally, in Figure 23, the histogram of primary turn angle magnitudes was centered around approximately 20°, while in Figure 27, the histogram of secondary turn angle magnitudes was centered around approximately 0°. These results demonstrate that MHC biobots are able to be significantly controlled during the first few seconds after stimulation. After about 2000 ms post-stimulation, the MHC biobots are able to be controlled less; this means that after 2000 ms post-stimulation, the MHC biobots turn in the contralateral direction much less often. Furthermore, because the histogram of secondary turn magnitudes (Figure 27) is centered around approximately 0° and not around approximately -20° as would be expected of a truly "corrective" turn, it is likely that the secondary turn is simply when the cockroach regains control of its motion rather than a "corrective" turn as noted in previous studies.

Average primary turn angles were found to be within 7.79° and 15.20°, which is fairly low compared to values found in previous work [5]. However, primary turns were calculated only using the first 2 seconds post-stimulation, whereas previous work has included larger timeframes. Rather than characterize MHC biobot motion in a large timeframe (~10 seconds), the goal of this study was to isolate and characterize primary and secondary turns. Furthermore, this study did not include stimulation of the cerci, which may have been a factor in the smaller turn angles observed. Average secondary turn angles were found to be within 0.05-11.06°, which illustrates that secondary turns were more often lower in magnitude or were in the ipsilateral direction of stimulation.

The antennae have generally been used to initialize turns in MHC biobots, while the cerci have generally been used to initialize forward motion. However, turning behavior of MHCs due to antennal stimulation cannot be completely decoupled from forward motion. Currently, there is no literature that demonstrates that antennal stimulation causes only turning motion, and cercal stimulation causes only forward motion. It is possible that there were effects caused by varied stimulus parameters, but they went unnoticed due the limited data collected in this study. In this study, only response rates, direction of turns, and turn angles were analyzed; all results demonstrated that stimulus voltage, duration, and the interaction of the two had no significant effects. However, it is still possible the stimulus parameters varied in this study affected MHC biobot motion in a capacity that was not analyzed in this study. It is possible to gather more information from the video files created in this study to determine if stimulus voltage, duration, or interaction of the two had effects unobserved in this study. Additional linear and angular motion data can be extracted from these videos, including distance traveled, linear velocity, linear acceleration, angular velocity, angular acceleration, and turn radius.

Most subjects showed a slight decrease in primary turn magnitude over time. Figure 29 shows an example of this phenomenon. Interestingly, this same phenomenon is not observed with secondary turns in most subjects, which excludes physical exhaustion as a possible explanation for the decrease in primary turn magnitudes. Figure 30 shows an example of this for Subject 16. It is possible that the MHC biobot is habituating to the stimulation over time by ignoring sensory input from its antennae and depending more on its other sensory feedback mechanisms. In addition, it is possible that there is some electrode-tissue interface breakdown, which reduces the electrode's ability to induce action potentials in the tissues. There also may be some level of permanent damage to the cockroaches' antennae neurons due to stimulation.

Based on these findings, there are several ways to improve MHC biobot technology. Most simply, researchers could limit the amount of time in between stimuli to approximately 2000 ms, which would ensure that most of the motion of the MHC biobots would result from stimuli and not the biobots own control. However, based on current literature, it is unclear if reducing the time between stimuli would cause an increase in MHC habituation to stimuli. Further studies should be conducted to determine if decreased time between stimuli affects the rate of habituation. Another method of improving MHC biobot technology is to use a feedback system, where the actual turn angle of an MHC biobot is measured. Then, when an MHC biobot begins to turn in the undesired direction, another stimulus could be applied.

As expected, high intrasubject and intersubject variability were observed in this study. This could be due to a multitude of reasons, including but not limited to temperature, humidity, time of day of the stimulation session, ambient light level, ambient noise level, placement of electrodes, MHC nutrition, and MHC physical exhaustion. Variability in MHC biobot motion is likely much larger than any effect due to stimulus amplitude or duration; therefore, more subjects

should be added in further studies in order to illuminate any possible effects of amplitude and duration on MHC biobot motion.

High temperatures and levels of humidity are associated with higher levels of motion in MHC, as these environmental characteristics closely mimic those of their natural environment. Because temperature and humidity were not controlled during stimulation sessions, it is possible that certain sessions were associated with higher levels of activity on a particularly warm or humid day. Furthermore, MHCs are nocturnal and are known to be more active at night. It is possible that stimulation sessions conducted later in the day may have resulted in higher MHC activity levels. Additionally, in American cockroaches, visual information converges on thoracic interneurons, which are also responsible for generating motor neuron signals. Assuming similar anatomies between the 2 cockroach species, it is possible that ambient light levels could have affected motor neuron signals and altered the motor output of the MHC biobot. MHCs often communicate through loud hisses; because the ambient noise level was not controlled, it is possible that the MHC biobots were responding to some sort of noise in addition to electrical stimulation during stimulation sessions. Further variability could have been introduced due to slightly different placement of electrodes. Though care was taken to ensure proper placement of the electrodes, it is difficult to ensure the electrodes are in exactly the same position. The same scenario is applicable to the placement of the ground electrode; it is difficult to ensure the ground electrode was in the same position for all subjects. Finally, MHC hydration and nutrition was not controlled and may have contributed to the high variability observed in this study.

## 6. LIMITATIONS

One limitation of this study was that the cerci were not stimulated along with the antennae due to limited stimulation equipment. It is likely that in commercial implementation of MHC biobot technology, the cerci would be stimulated as previous work has shown that stimulation of the antennae and cerci initiates significant motion. However, with the equipment used, only 1 electrode was able to be stimulated at a time. With more time and resources, the cerci would also be stimulated.

This experiment also utilized tethered stimulus electronics. Outside of a laboratory setting, a fully-implemented MHC biobot would utilize a wireless electronic backpack. Therefore, the MHC biobots in this study may have behaved differently (i.e., altered gait, slower, etc.) with a larger weight on their back due to an electronic backpack.

One of the assumptions of this study was that if the subjects were in control of their motion, they would turn 50% in the contralateral direction to stimuli and 50% in the ipsilateral direction. However, no data was collected to support this assertion. It is possible that the MHCs turned in a specific direction more often in the laboratory due to variability in light, smell, heat, etc. In future tests, this assumption should be tested by placing the MHC in the experimental set-up several times prior to providing stimulation and noting the frequency in which the MHC turns in each direction. The resulting percentage of turns in each direction can then be used as a baseline to compare the percentage of turns in the contralateral direction following stimulation.

A final limitation is the relatively small sample size used in this study. With additional time and resources, more subjects would be included which would allow for a higher degree of certainty in the results.

**7. CONCLUSION**

This study has developed an improved motion profile in response to neurostimulation of

MHC biobot antennae by characterizing the 2-phase turning response of MHC biobots.

Furthermore, this study has demonstrated that modulation of amplitude and duration of the

applied electrical stimuli does not affect the responsiveness, direction of, or magnitude of turn

angle of MHC biobots for both the primary and secondary turns.  MHC biobots are able to be

significantly controlled during the primary turn.  However, MHC biobots are not able to be

significantly controlled during the secondary turn.  The secondary turn is likely when the

cockroach regains control of its motion rather than a "corrective" turn as noted in previous

studies.  To improve MHC biobot technology, researchers could limit the amount of time

between stimuli to approximately 2000 ms or introduce a feedback system where actual turn

angle is measured, and stimuli are applied when the MHC biobot begins turning in the undesired

direction.

**8. FUTURE WORK**

Future research on MHC biobots should focus on increasing response rates and reducing habituation rates. One promising method of reducing habituation rates is to use a motor neuron pathway rather than a sensory neuron pathway to direct MHC biobot motion. Specifically, similarly to the study by Sanchez et al. using American cockroaches, it should be investigated if stimulation of the prothoracic ganglia can direct MHC biobot motion [18]. Because this method uses motor neurons, it would likely be less susceptible to habituation, as MHCs can easily learn to ignore sensory feedback from the antennae.

One of the main applications for MHC biobots is in search and rescue operations. In certain search and rescue scenarios such as a crumbled building at night, it will likely be much colder than room temperature. It is widely known that MHCs prefer higher temperatures and humidity, but it has not been studied how MHC biobots behave in controlled lower temperatures. Therefore, additional research should be conducted to determine if it is possible to direct MHC biobot motion at lower temperatures. Furthermore, additional research should be conducted to evaluate how temperature affects MHC biobot motion.

To reduce the time and cost of performing multiple insect surgeries, an option is to use the same MHC subject over a period of multiple days. However, the rate of habituation is unknown after an MHC subject is given a "recovery period." Further studies should focus on determining if MHC biobots can be used for multiple sessions and what the effects of a "recovery period" are on MHC motion and habituation.

# LIST OF REFERENCES

[1] I. S. science editor, "Cockroach robots? Not nightmare fantasy but science lab reality," *The Guardian*, 04-Mar-2015.

[2] H. Sato *et al.*, "Remote Radio Control of Insect Flight," *Front Integr Neurosci*, vol. 3, Oct. 2009.

[3] T. Moore et al., "Directed Locomotion in Cockroaches: "Biobots"," *Acta Entomologica Slovenica,* vol. 6, no. 2, pp. 71-78, Dec 1998.

[4] T. Latif and A. Bozkurt, "Line following terrestrial insect biobots," *Conf Proc IEEE Eng Med Biol Soc*, pp. 972–975, 2012.

[5] "Effective Stimulus Parameters for Directed Locomotion in Madagascar Hissing Cockroach Biobot." [Online]. Available: https://journals.plos.org/plosone/article?id=10.1371/journal.pone.0134348. [Accessed: 13-Jul-2019].

[6] "'Biobot' Cyborg Cockroaches Could Be The Future Of Disaster Relief | Inverse." [Online]. Available: https://www.inverse.com/article/23957-cyborg-biobot-cockroaches. [Accessed: 13-Jul-2019].

[7] E. Whitmire, T. Latif, and A. Bozkurt, "Acoustic sensors for biobotic search and rescue," in *IEEE SENSORS 2014 Proceedings*, Valencia, Spain, 2014, pp. 2195–2198.

[8] "Bug Biobots: Drones and Insect Biobots to Map Disaster Areas : News : Nature World News." [Online]. Available: https://www.natureworldnews.com/articles/32313/20161119/bug-biobots-drones-insect-map-disaster-areas.htm. [Accessed: 13-Jul-2019].

[9] "The RoboRoach Bundle." [Online]. Available: https://backyardbrains.com/products/roboroach. [Accessed: 13-Jul-2019].

[10] "Microrobotics: Present, challenges, perspectives - IEEE Conference Publication." [Online]. Available: https://ieeexplore.ieee.org/abstract/document/7090614. [Accessed: 13-Jul-2019].

[11] F. Cao *et al.*, "A Biological Micro Actuator: Graded and Closed-Loop Control of Insect Leg Motion by Electrical Stimulation of Muscles," *PLoS One*, vol. 9, no. 8, Aug. 2014.

[12] N. J. Kohut, P. M. Birkmeyer, K. C. Peterson, and R. S. Fearing, "Maneuverability and mobility in palm-sized legged robots," presented at the SPIE Defense, Security, and Sensing, Baltimore, Maryland, USA, 2012, p. 83731I.

[13] A. Hoover, S. Burden, X.-Y. Fu, S. Sastry, and R. S. Fearing, "Bio-inspired design and dynamic maneuverability of a minimally actuated six-legged robot," presented at the 2010 3rd IEEE RAS and EMBS International Conference on Biomedical Robotics and Biomechatronics, BioRob 2010, 2010, pp. 869–876.

[14] A. Bozkurt, R. F. Gilmour, and A. Lal, "Balloon-Assisted Flight of Radio-Controlled Insect Biobots," *IEEE Transactions on Biomedical Engineering*, vol. 56, no. 9, pp. 2304–2307, Sep. 2009.

[15] T. V. Truong, D. Byun, L. C. Lavine, D. J. Emlen, H. C. Park, and M. J. Kim, "Flight behavior of the rhinoceros beetleTrypoxylus dichotomusduring electrical nerve stimulation," *Bioinspir. Biomim.*, vol. 7, no. 3, p. 036021, Jun. 2012.

[16] S. L Giampalmo *et al.*, "Generation of complex motor patterns in american grasshopper via current-controlled thoracic electrical interfacing," *Conference proceedings : ... Annual International Conference of the IEEE Engineering in Medicine and Biology Society. IEEE Engineering in Medicine and Biology Society. Conference*, vol. 2011, pp. 1275–8, Aug. 2011.

[17] "DragonflEye uses dragonfly cyborgs for guided pollination, payload delivery, reconnaissance and even precision medicine and diagnostics," *Innovation Toronto*, 31-Jan-2017.

[18] C. J. Sanchez, C.-W. Chiu, Y. Zhou, J. M. González, S. B. Vinson, and H. Liang, "Locomotion control of hybrid cockroach robots," *J R Soc Interface*, vol. 12, no. 105, Apr. 2015.

[19] "Biobots, Roll Out! | DiscoverMagazine.com." [Online]. Available: http://discovermagazine.com/2016/april/7-biobots-roll-out. [Accessed: 13-Jul-2019].

[20] "Scientists Wire Up Live Beetles To Serve As Robots In Singapore - News Punch." [Online]. Available: https://newspunch.com/scientists-wire-up-live-beetles-to-serve-as-robots-in-singapore/. [Accessed: 13-Jul-2019].

[21] "Madagascar Hissing Cockroach | Department of Entomology." [Online]. Available: https://entomology.unl.edu/madagascar-hissing-cockroach. [Accessed: 13-Jul-2019].

[22] "Remote Controlled Cockroach Biobots." [Online]. Available: https://scitechdaily.com/remote-controlled-cockroach-biobots/. [Accessed: 13-Jul-2019].

[23] "Cockroach Care Sheet | Petco." [Online]. Available: https://www.petco.com/content/petco/PetcoStore/en_US/pet-services/resource-center/caresheets/cockroach-care-sheet.html. [Accessed: 13-Jul-2019].

[24] "Madagascar Hissing Cockroaches: Information and Care," *OSU Fact Sheets*. [Online]. Available: http://factsheets.okstate.edu/documents/l-278-madagascar-hissing-cockroaches-information-and-care/. [Accessed: 13-Jul-2019].

[25] "Figure 1. External anatomy of male and female Madagascar hissing...," *ResearchGate*. [Online]. Available: https://www.researchgate.net/figure/External-anatomy-of-male-and-female-Madagascar-hissing-cockroaches-including-leg_fig1_279041039. [Accessed: 13-Jul-2019].

[26] J. Okada, "Cockroach antennae," *Scholarpedia*, vol. 4, no. 10, p. 6842, Oct. 2009.

[27] "Neuroethology: Escape Behavior in the Cockroach." [Online]. Available: http://nelson.beckman.illinois.edu/courses/neuroethol/models/cockroach_escape/roach_escape.html. [Accessed: 13-Jul-2019].

[28] C. A. McGorry, C. N. Newman, and J. D. Triblehorn, "Neural responses from the wind-sensitive interneuron population in four cockroach species," *J Insect Physiol*, vol. 66, pp. 59–70, Jul. 2014.

[29] D. Harnack, C. Winter, W. Meissner, T. Reum, A. Kupsch, and R. Morgenstern, "The effects of electrode material, charge density and stimulation duration on the safety of high-frequency stimulation of the subthalamic nucleus in rats," *J. Neurosci. Methods*, vol. 138, no. 1–2, pp. 207–216, Sep. 2004.

[30] D. A. Wagenaar, J. Pine, and S. M. Potter, "Effective parameters for stimulation of dissociated cultures using multi-electrode arrays," *J. Neurosci. Methods*, vol. 138, no. 1–2, pp. 27–37, Sep. 2004.

[31] "Madagascar hissing cockroach," *Oregon Zoo*. [Online]. Available: https://www.oregonzoo.org/discover/animals/madagascar-hissing-cockroach. [Accessed: 13-Jul-2019].

[32] "RoboRoach Experiment #1 – Neural Interface Surgery," *Roboroach*. [Online]. Available: https://backyardbrains.com/experiments/files/RoboRoachExperiment-NeuralInterfaceSurgery.pdf. [Accessed: 13-Jul-2019].

[33] "Kinovea." [Online]. Available: https://www.kinovea.org/features.html. [Accessed: 13-Jul-2019].

**APPENDICES**

Appendix A: Subject Physical Characteristics Data

Appendix B: Raw Cumulative Turn Angle Data

# APPENDIX A: Subject Physical Characteristics Data

**Table A1.** Subject physical characteristics, including sex, weight, length, width, height, and antennae used for stimulation.

| Subject # | Sex | Weight (g) | Length (mm) | Width (mm) | Height (mm) | Antennae |
|---|---|---|---|---|---|---|
| 1 | Male | 7.28 | 60.27 | 22.38 | 15.97 | Both |
| 2 | Male | 7.65 | 59.03 | 20.96 | 16.18 | Both |
| 3 | Male | 7.79 | 58.55 | 21.73 | 16.73 | Both |
| 4 | Male | 7.32 | 58.18 | 22.43 | 16.83 | Left |
| 5 | Male | 7.77 | 60.77 | 25.88 | 17.84 | Both |
| 6 | Male | 7.18 | 56.19 | 23.61 | 14.88 | Both |
| 7 | Male | 7.36 | 62.04 | 21.84 | 17.14 | Both |
| 8 | Male | 7.1 | 58.36 | 22.84 | 15.83 | Both |
| 9 | Male | 6.54 | 52.4 | 23.74 | 15.35 | Both |
| 10 | Male | 7.61 | 57.58 | 23.02 | 16.89 | Both |
| 11 | Male | 7.77 | 58.76 | 21.19 | 16.34 | Both |
| 12 | Female | 9.56 | 66.31 | 24.07 | 16.99 | Both |
| 13 | Male | 6.35 | 57.27 | 22.26 | 14.76 | Both |
| 14 | Female | 10.24 | 70.96 | 25.86 | 17.07 | Both |
| 15 | Male | 7.51 | 61.23 | 22.63 | 16.72 | Both |
| 16 | Male | 7.05 | 57.69 | 20.57 | 16.29 | Left |
| 17 | Female | 9.86 | 67.31 | 24.14 | 17.02 | Both |
| 18 | Male | 6.19 | 56.94 | 22.48 | 15.27 | Both |
| 19 | Male | 7.25 | 60.84 | 22.56 | 16.79 | Both |
| 20 | Male | 7.52 | 60.93 | 22.49 | 17.39 | Both |

# APPENDIX B: Raw Cumulative Turn Angle Data

**Figure B1.** Raw cumulative turn angle data for all subjects under the following stimulus pulse parameters: 1 V and 0.5 s. Data from subjects 13, 17, and 18 are not included, as these subjects were not responsive to any antennal stimulation.
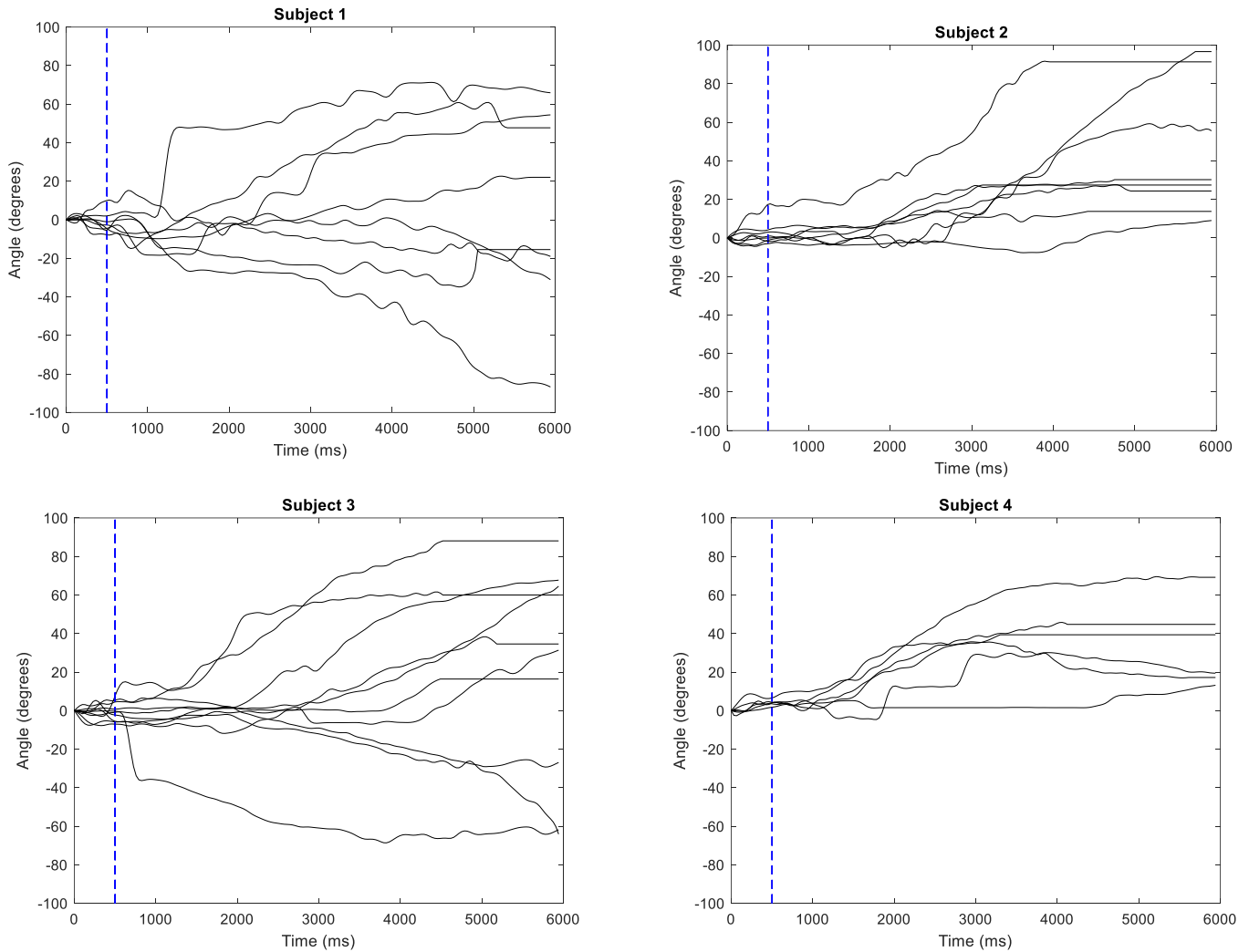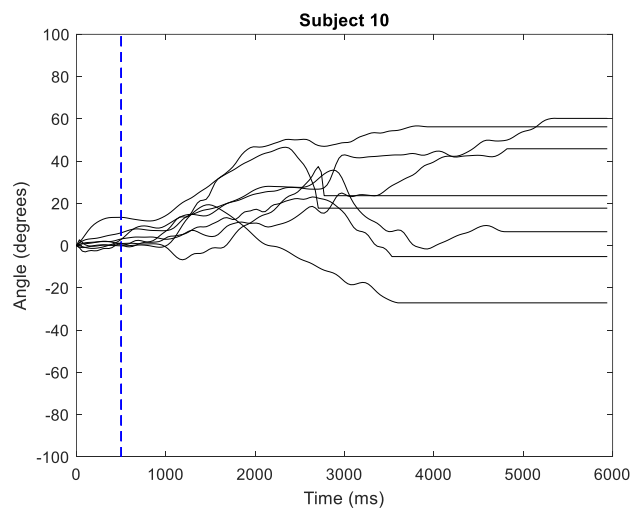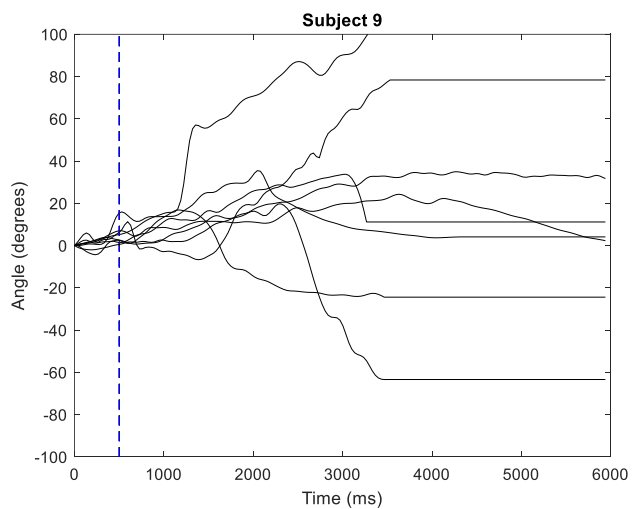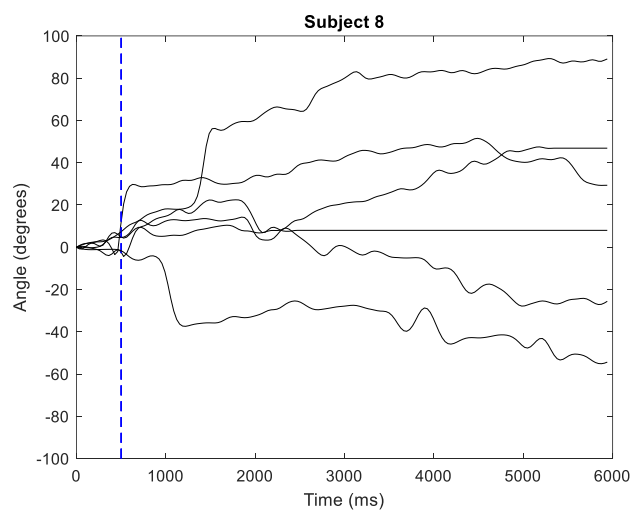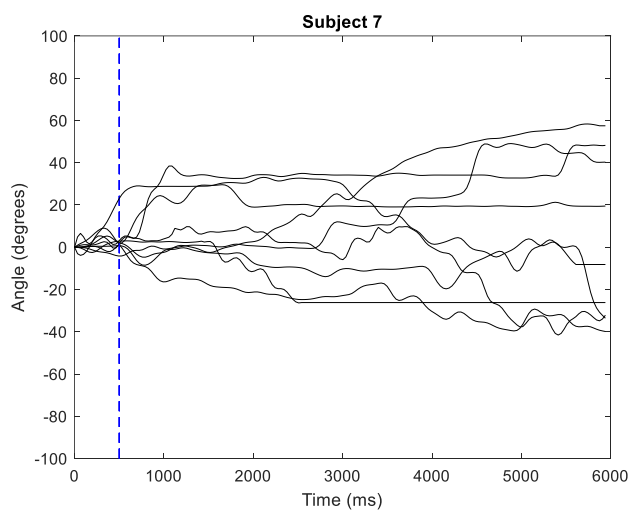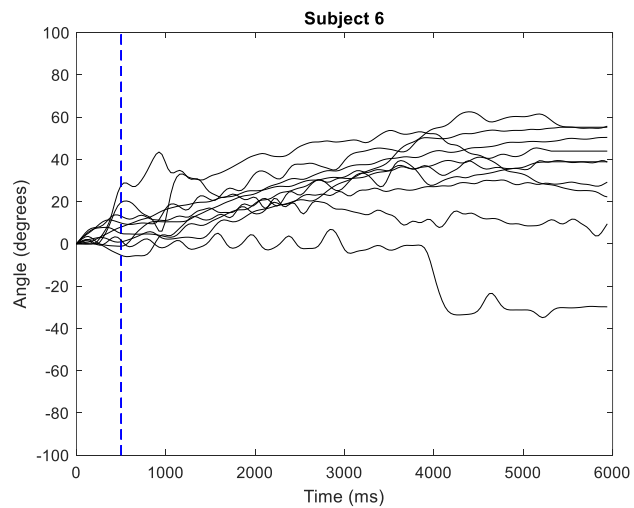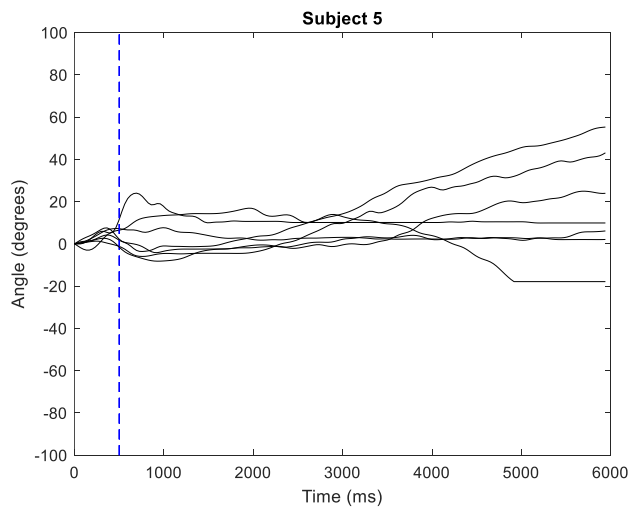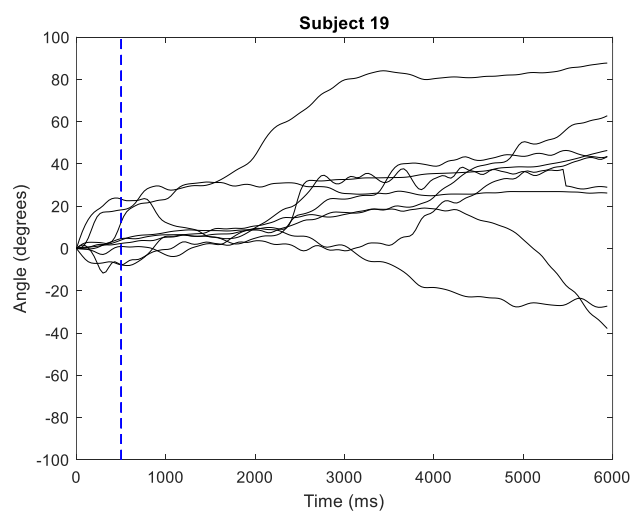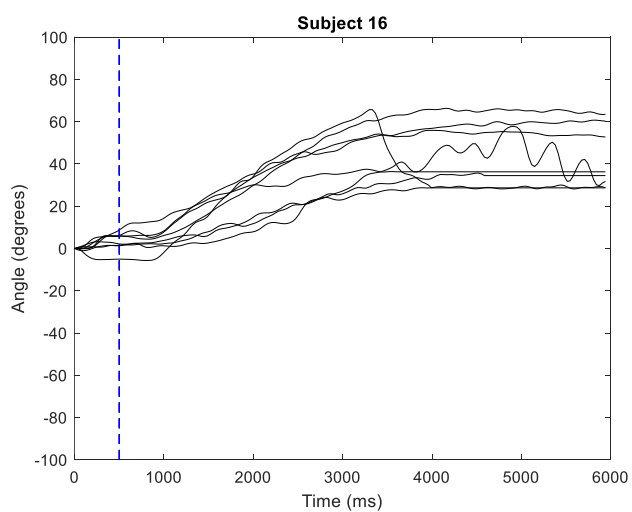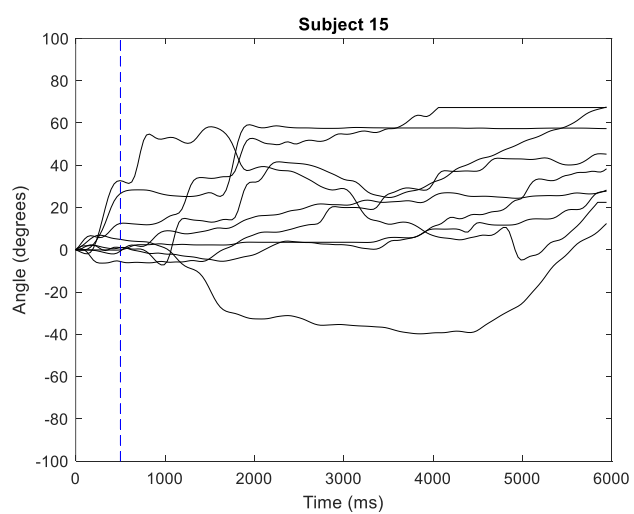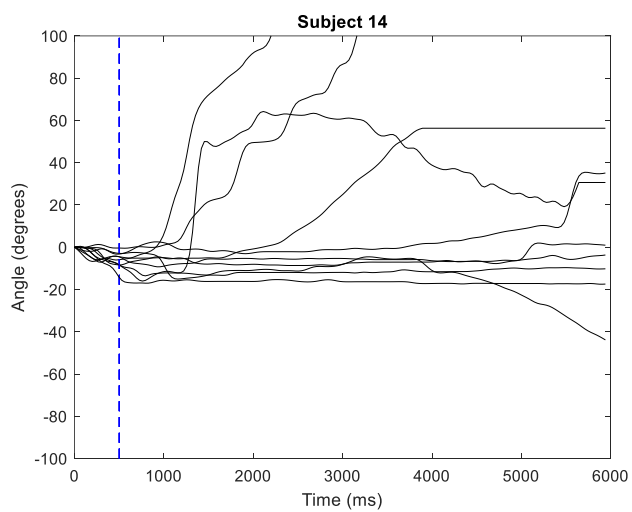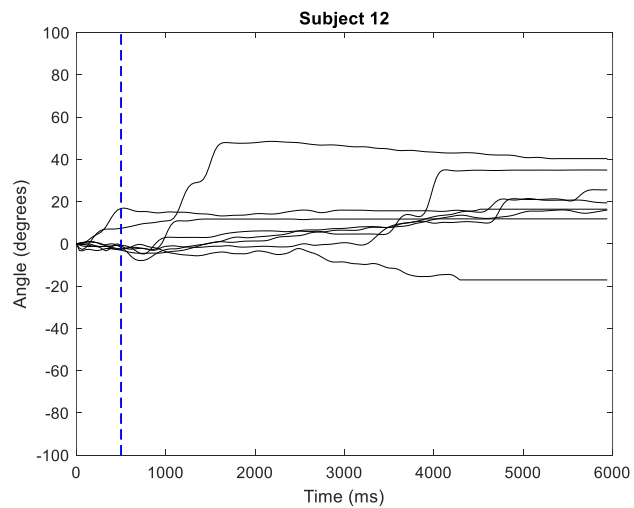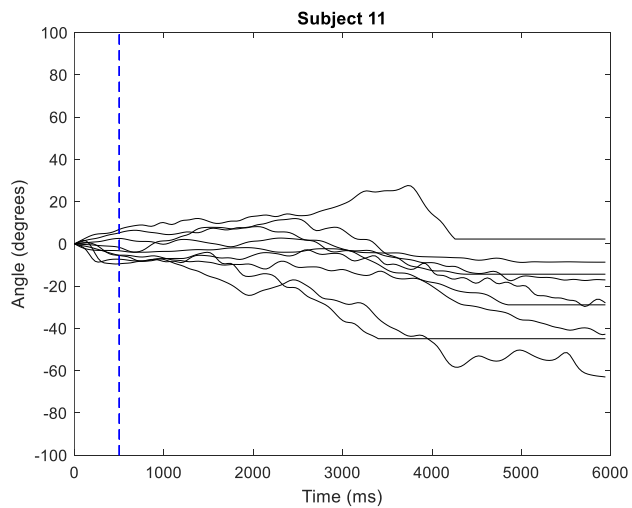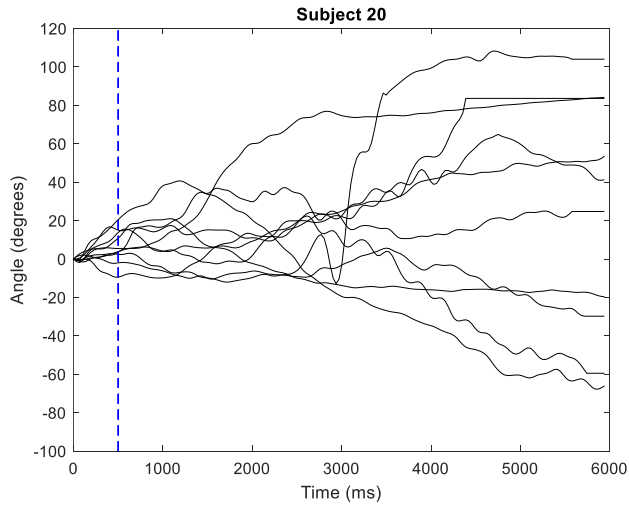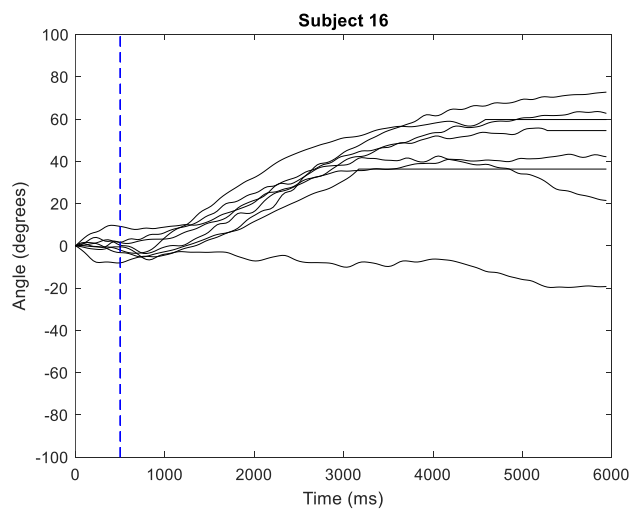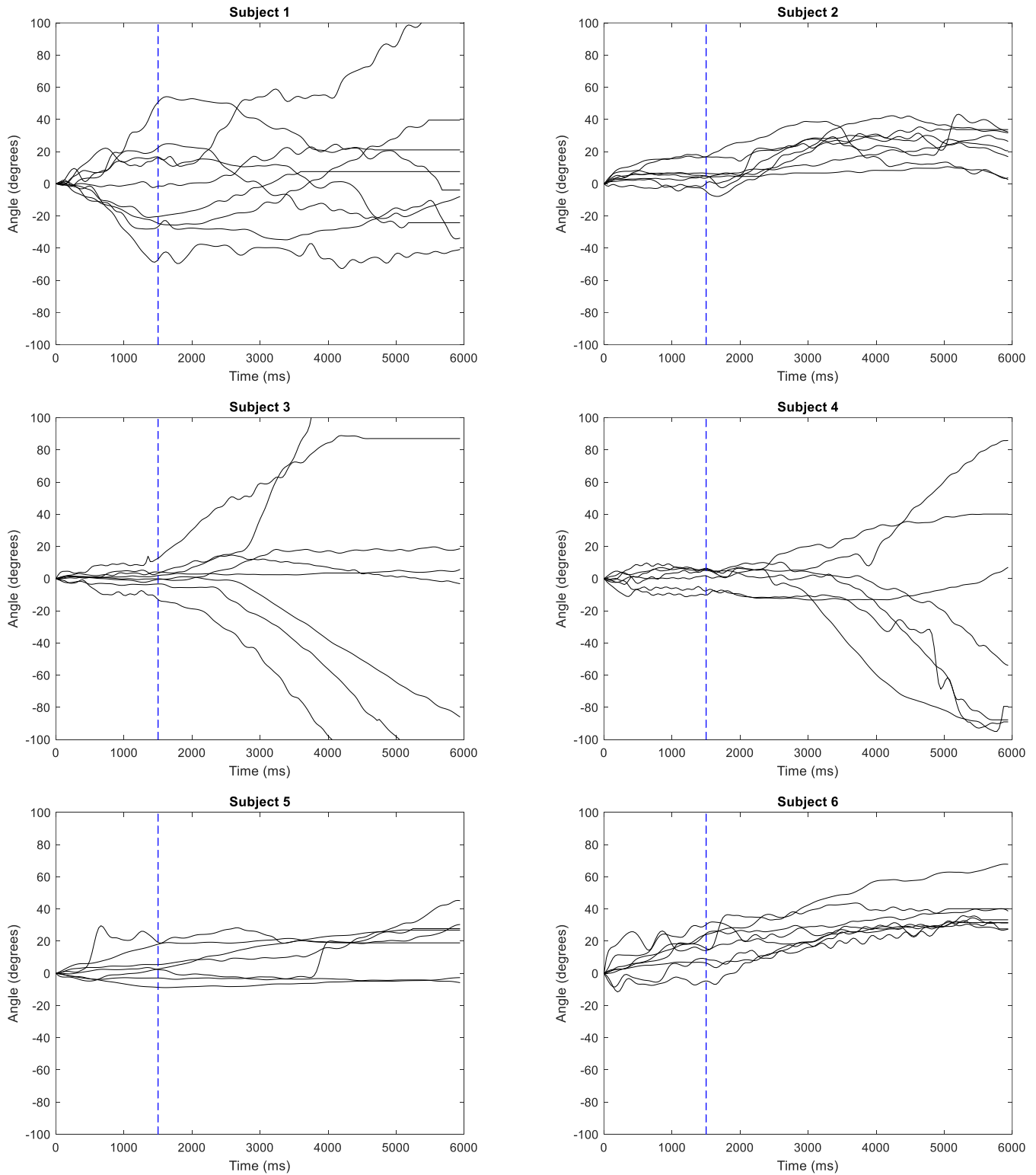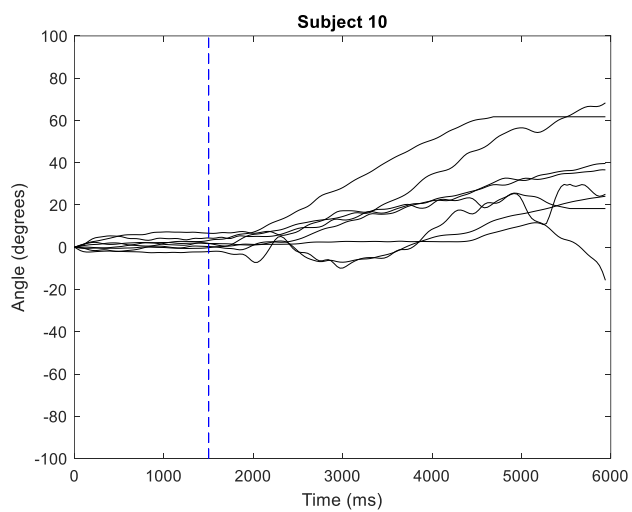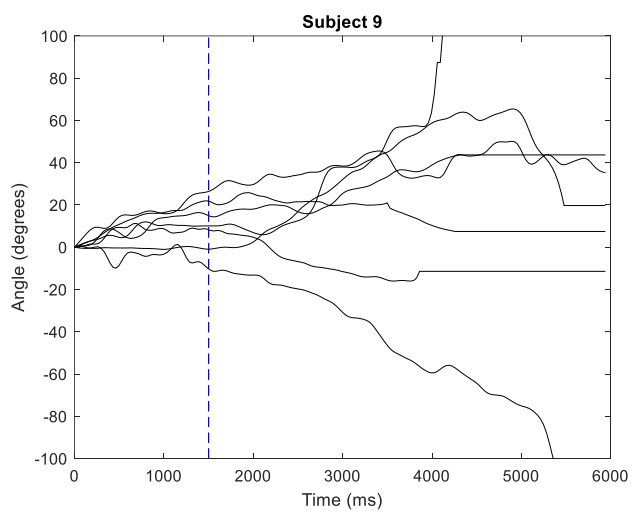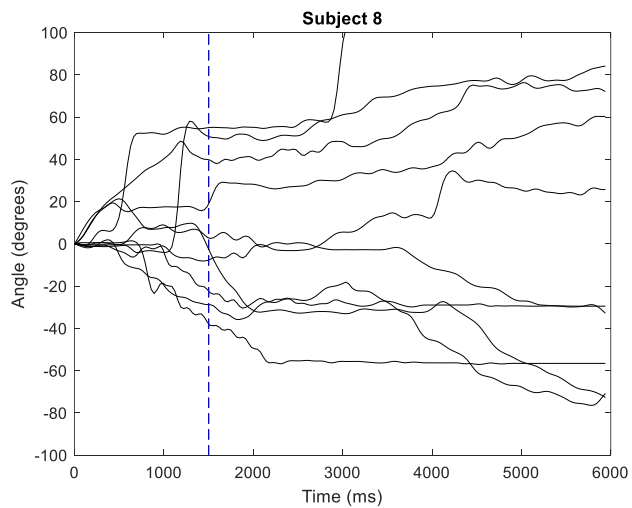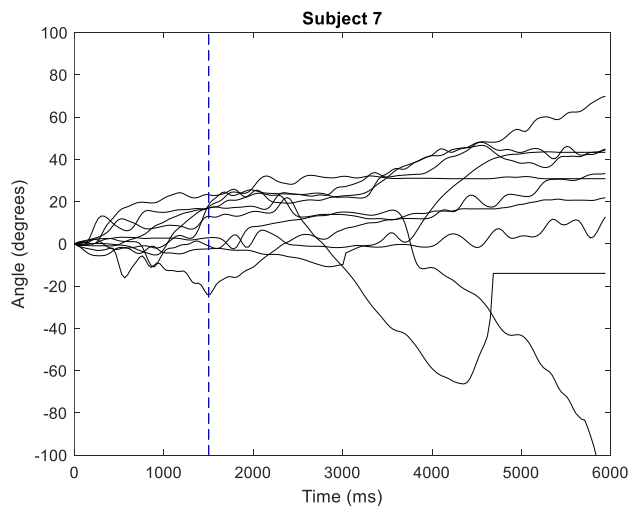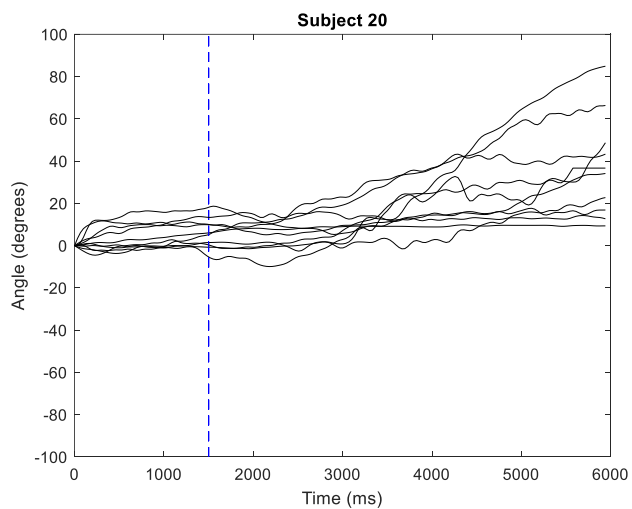
**Figure B2.** Raw cumulative turn angle data for all subjects under the following stimulus pulse parameters: 3 V and 0.5 s.  Data from subjects 13, 17, and 18 are not included, as these subjects were not responsive to any antennal stimulation.
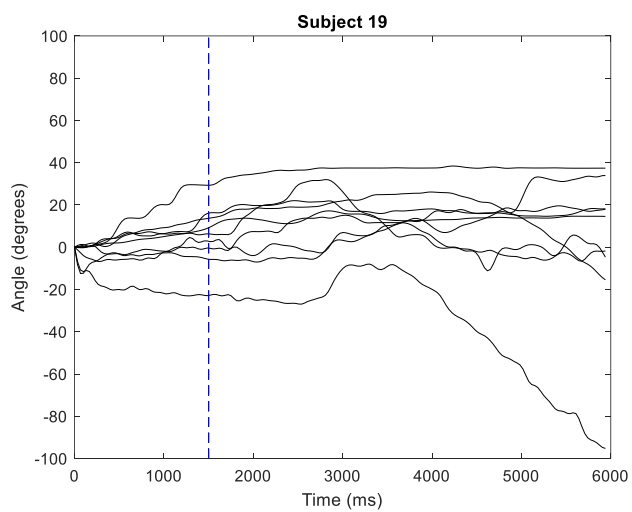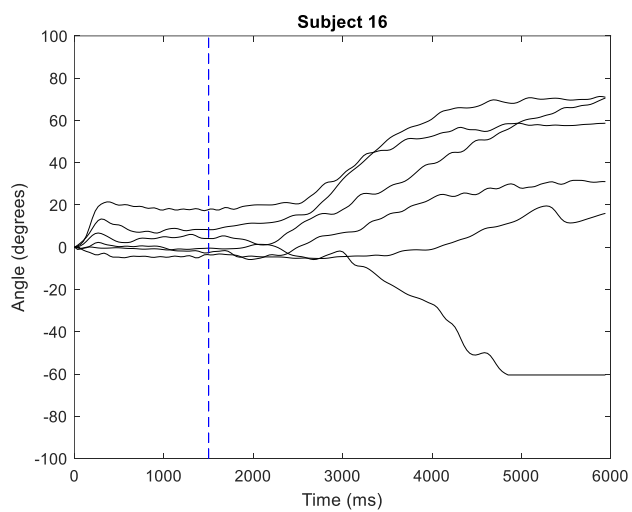
Subject 16



Subject 19
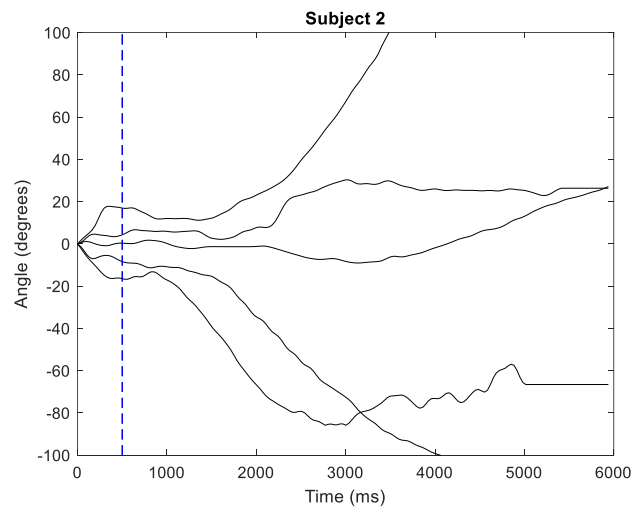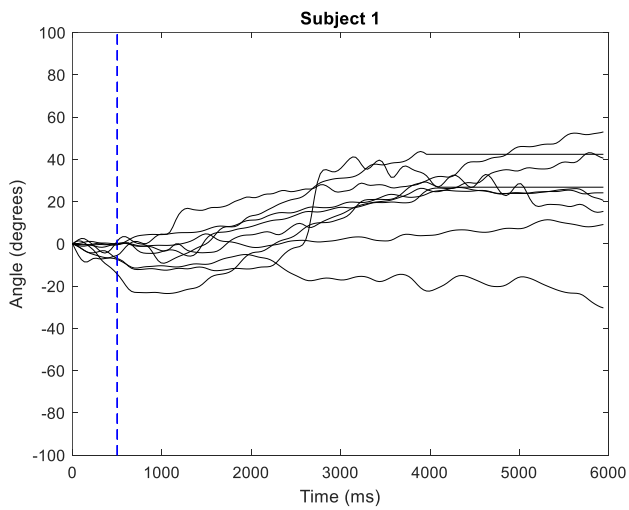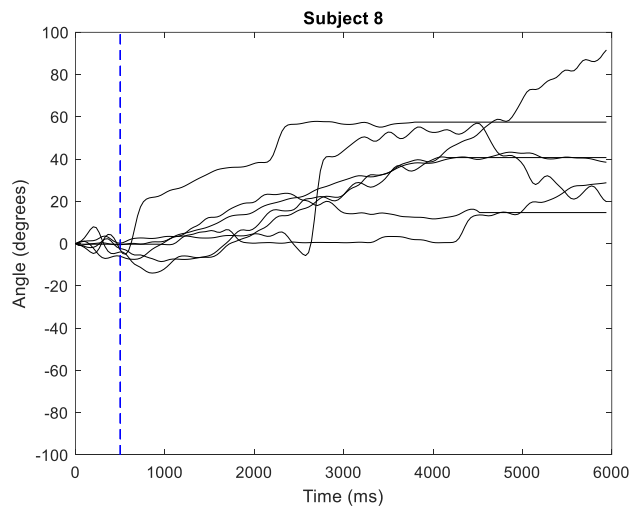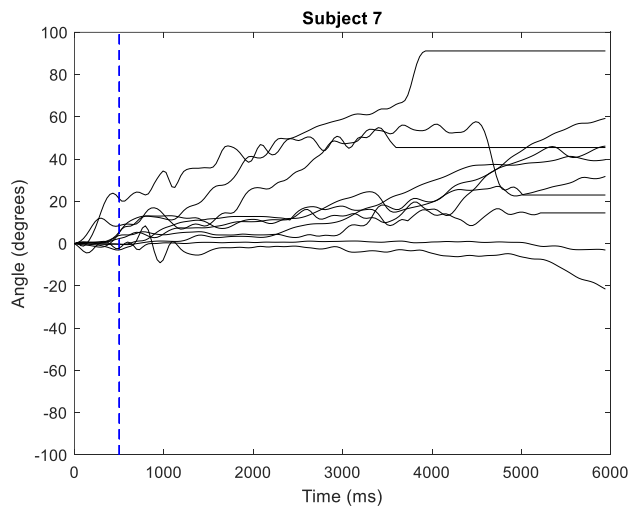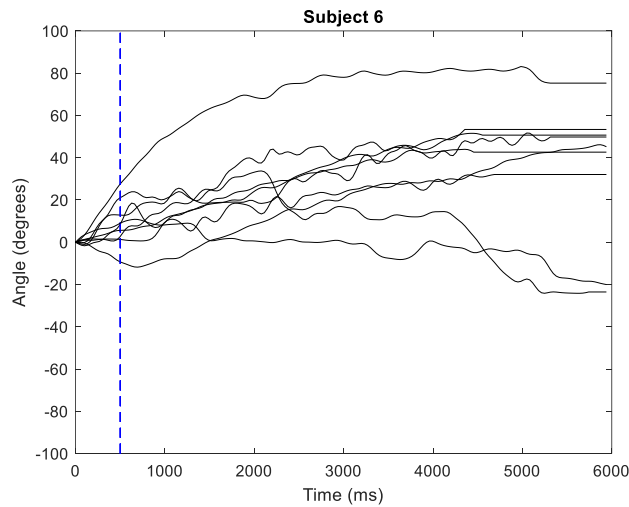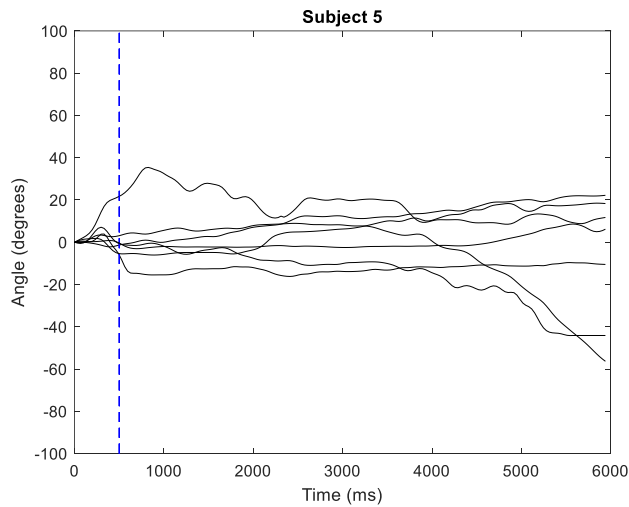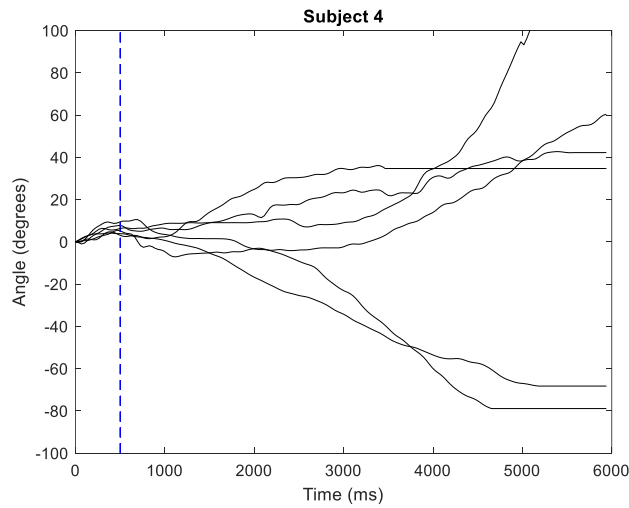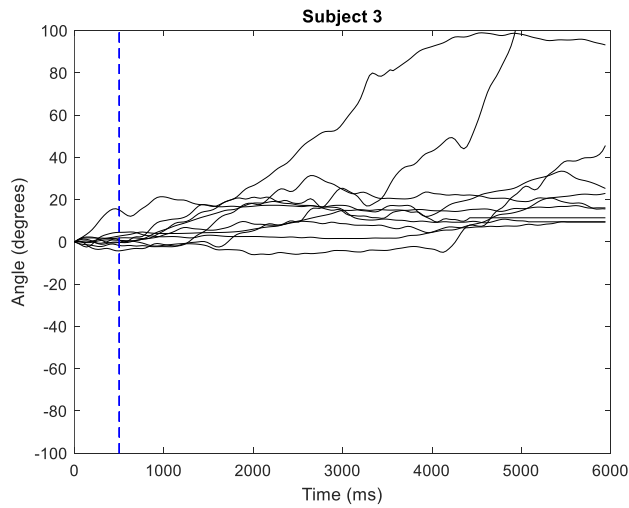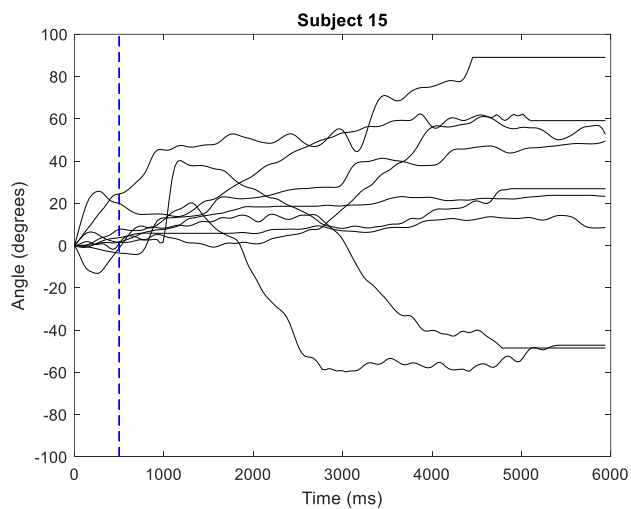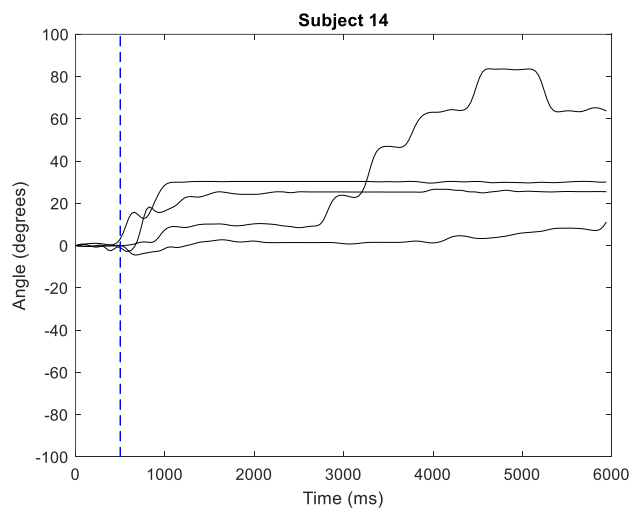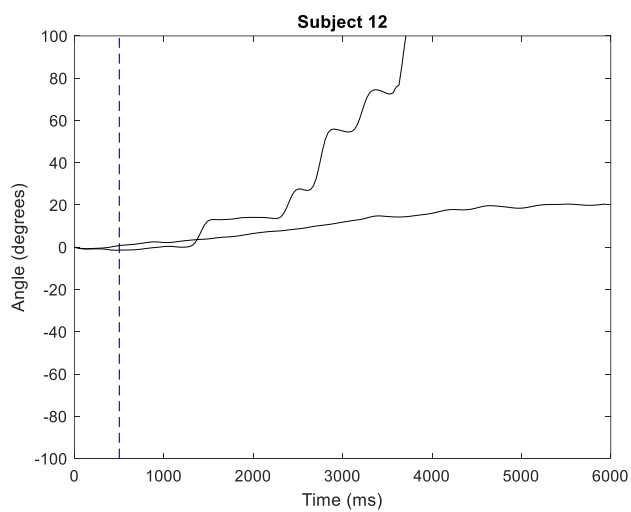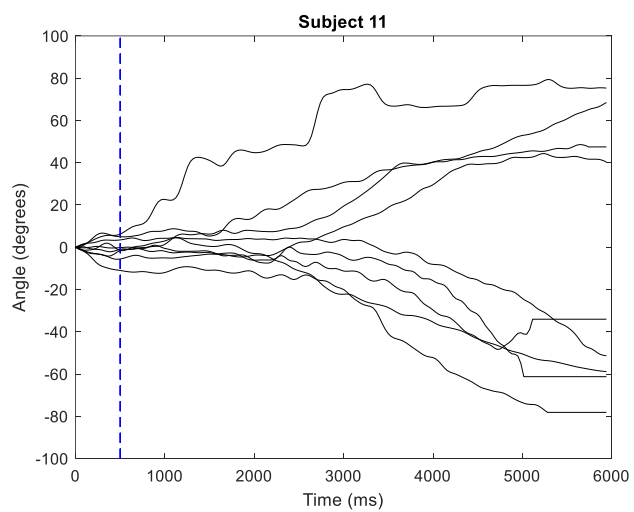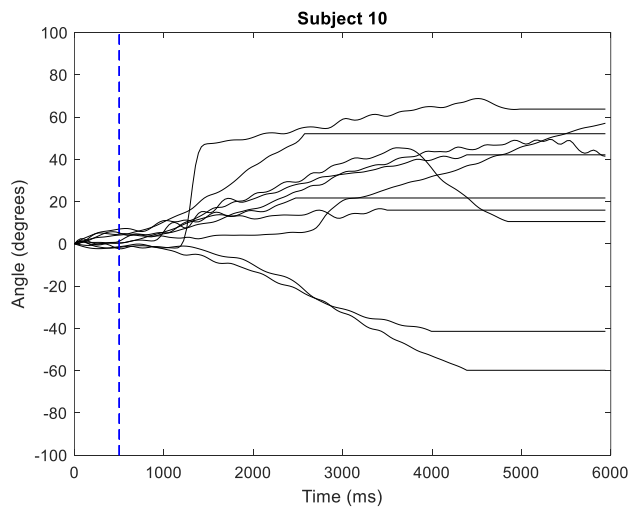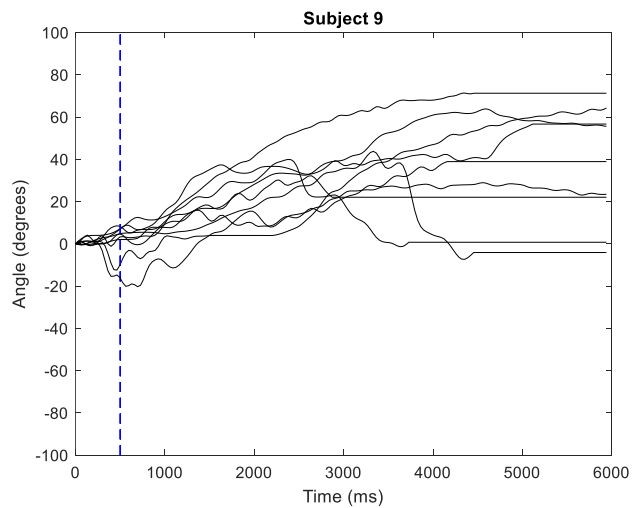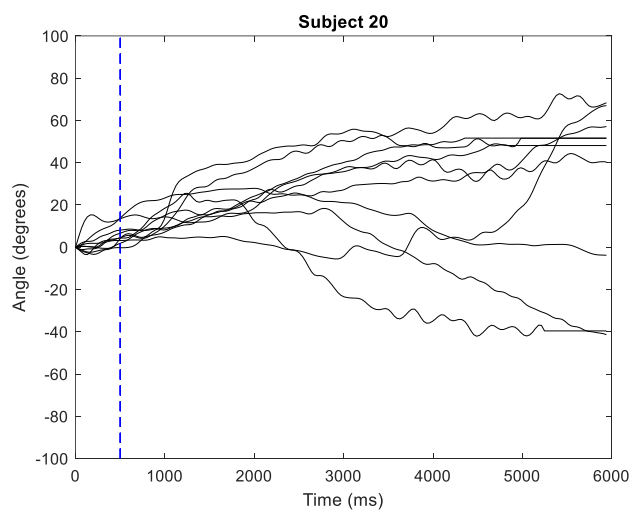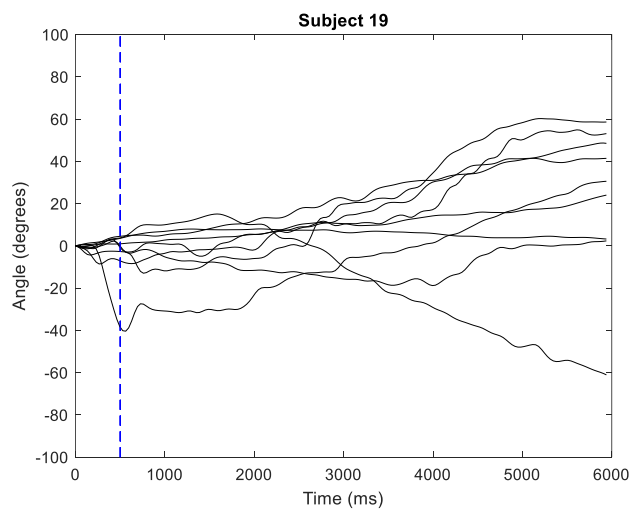


Subject 20

**Figure B3.** Raw cumulative turn angle data for all subjects under the following stimulus pulse parameters: 1 V and 1.5 s.  Data from subjects 13, 17, and 18 are not included, as these subjects were not responsive to any antennal stimulation.
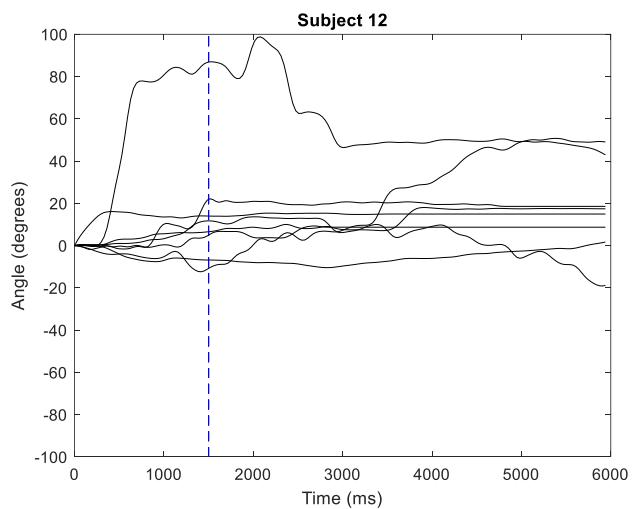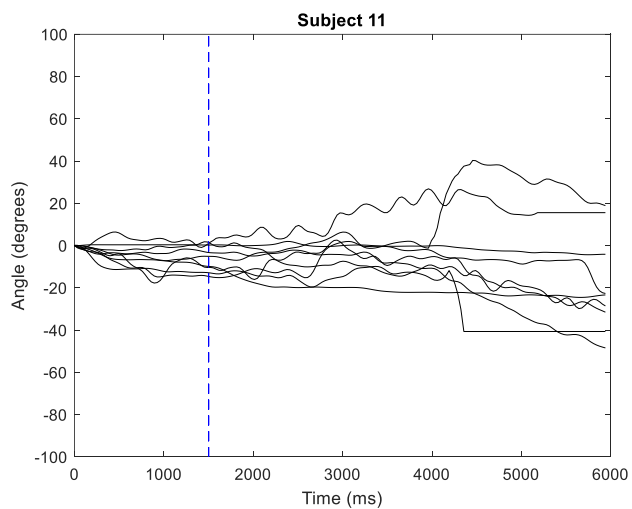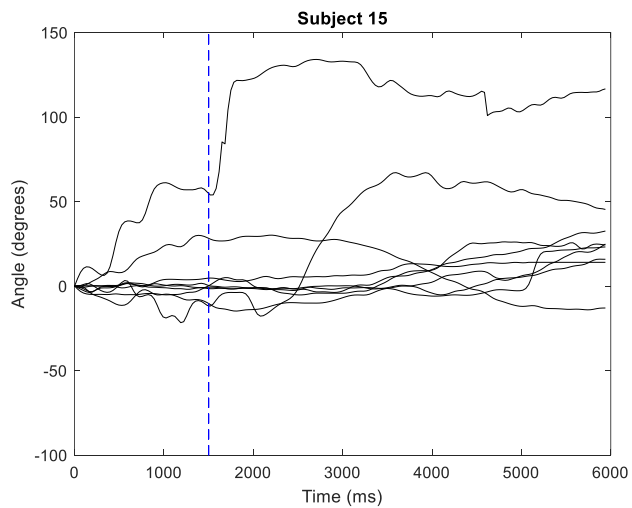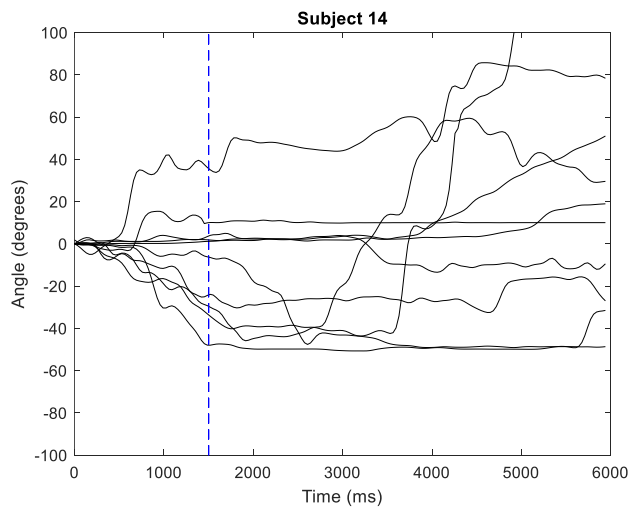
**Figure B4.** Raw cumulative turn angle data for all subjects under the following stimulus pulse parameters: 3 V and 1.5 s. Data from subjects 13, 17, and 18 are not included, as these subjects were not responsive to any antennal stimulation.